Composition of Primary Postcumulus Amphibole and Phlogopite Within an Olivine Cumulate in the Stillwater Complex, Montana

U.S. GEOLOGICAL SURVEY BULLETIN 1674–A

Chapter A

Composition of Primary Postcumulus Amphibole and Phlogopite Within an Olivine Cumulate in the Stillwater Complex, Montana

By NORMAN J PAGE and MICHAEL L. ZIENTEK

U.S. GEOLOGICAL SURVEY BULLETIN 1674

CONTRIBUTIONS ON ORE DEPOSITS IN THE EARLY MAGMATIC ENVIRONMENT

DEPARTMENT OF THE INTERIOR
DONALD PAUL HODEL, Secretary

U.S. GEOLOGICAL SURVEY
Dallas L. Peck, Director

UNITED STATES GOVERNMENT PRINTING OFFICE, WASHINGTON : 1987

For sale by the
Books and Open-File Reports Section
U.S. Geological Survey
Federal Center, Box 25425
Denver, CO 80225

Library of Congress Cataloging-in-Publication Data

Page, Norman J
Composition of primary postcumulus amphibole and phlogopite within an olivine cumulate in the Stillwater Complex, Montana.

(Contributions on ore deposits in the early magmatic environment; A)
(U.S. Geological Survey Bulletin 1674–A)
Bibliography
Supt. of Docs. No.: I 19.3:1674–A
1. Amphiboles—Montana. 2. Phlogopite—Montana. 3. Chrysolite—Montana.
I. Zientek, Michael L. II. Title. III. Series. IV. Series: U.S. Geological Survey Bulletin 1674–A.

QE75.B9 No. 1674–A	557.3 s	86-600291
[QE391.A53]	[549'.6]	

CONTENTS

FIGURES

TABLES

The use of trade names in this report is for descriptive purposes only and does not constitute endorsement by the U.S. Geological Survey.

Composition of Primary Postcumulus Amphibole and Phlogopite Within an Olivine Cumulate in the Stillwater Complex, Montana

By Norman J Page *and* Michael L. Zientek

Abstract

Postcumulus amphibole and phlogopite from an olivine cumulate of cyclic unit 2 in the Archean Stillwater Complex, Montana, containing the B-chromitite, were analyzed with an electron microprobe. The brown amphiboles are pargasite or pargasitic hornblendes containing as much as 4.5 weight percent TiO_2 and 1.8 weight percent Cr_2O_3, and they are compositionally zoned. Three distinct textural occurrences were noted: (1) as material rimming chromite but not replacing pyroxene, (2) as interstitial material replacing augite but not in contact with chromite, and (3) as interstitial material in rocks that contain no cumulus spinel. Cation-cation plots show that most of the coupled substitutions are of tschermakitic and edenitic type, and that hornblendes in category (3) are distinct from those in categories (1) and (2) in not having substitutions including Na in the M_4 site and in having lower contents of Ti and Cr. Hornblendes associated with chromite have a larger extent of coupled substitution than those associated with augite and may be slightly more magnesium rich. However, the large extent of coupled substitution is not reflected by systematic increases in any one of the elements involved in the coupled substitution (that is, Al^{IV}, Ti, or Cr). Variations in compositions of zoned crystals in contact with chromite, pyroxene, olivine, and plagioclase support this observation, with the crystals having higher cation units of Ti, Cr, and Al^{IV} when the hornblende is in contact with chromite. Variations in the composition of hornblende with stratigraphic position allow the size-graded olivine cumulate package of units to be divided into three parts. The lower part has complex increasing and decreasing trends of $Mg/(Mg + Fe^{2+})$ (with an average ratio of 0.82), increasing upward Ti, Al^{IV}, and Cl contents, decreasing upward F content, and constant Cr content. Hornblende from the middle part, which contains the B-chromitite, has slightly higher $Mg/(Mg + Fe^{2+})$, about 0.83 to 0.84, with Ti increasing upward. The upper part, a portion of which contains no cumulus chromite, has lower $Mg/(Mg + Fe^{2+})$, approximately 0.81, with Cr and Ti increasing upward. Nominal crystallization temperatures of hornblendes based on their Al^{IV} contents range from 905 to 981 °C and average about 930 °C. Single zoned crystals appear to record a range of temperatures, with higher temperatures (980 °C) near chromite and lower temperatures (930–940 °C) away from chromite.

Phlogopite has a narrow range of composition (approximately 70 to 80 percent phlogopite end member) and substitutions that involve about equal amounts of annite and siderophyllite. The phlogopite has TiO_2 greater than 3.0 weight percent (with two exceptions) and Cr_2O_3 contents up to 1.5 weight percent. Variations in composition with stratigraphic position similar to those of the hornblendes are observed. It is not yet possible to suggest the conditions under which phlogopite crystallized except to conjecture that these conditions must have been similar to those prevailing when the hornblendes crystallized.

The textural and chemical evidence indicate that the hornblendes crystallized from trapped interstitial liquids at high temperatures. The variation in compositions suggests that the coexisting crystalline assemblage influenced the hornblende composition. Large-scale movement (greater than centimeters) of trapped liquid, which would homogenize the final hornblende compositions, did not occur or had ceased by the time the hornblende crystallized. The low contents of Cl and F in both phlogopites and hornblendes indicate that the magma was not noticeably enriched in these elements, nor is there any positive evidence for these volatiles streaming up through the olivine cumulate to concentrate base and precious metals.

INTRODUCTION

Numerous studies of cyclic units in the Peridotite zone of the Ultramafic series[1] of the Archean Stillwater Complex have examined the petrologic, mineralogic, and geochemical characteristics of the cumulus minerals (Jackson, 1961, 1963, 1967, 1968, 1969, 1970, 1971; Page and others, 1972; Raedeke, 1982; Raedeke and McCallum, 1982a, b, 1984). However, the postcumulus (interstitial) minerals have not been studied in the same detail. Therefore, this investigation focuses on postcumulus amphibole and phlogopite from olivine cumulates containing a chromite seam; this unit has been correlated with cyclic unit 2 in the Stillwater Complex, which contains the B-chromitite (Jackson, 1963, 1968). The unit was selected because it contains an olivine cumulate in which the mineralogic, petrologic, and geochemical details of the cumulus minerals and their alteration are documented in detail (Page and others, 1972; Page, 1976; Page and

[1]The stratigraphic terminology for the Stillwater Complex follows that of Zientek and others (1985).

others, 1976). The comparative simplicity of this unit should reduce the number of assemblages to evaluate, even though experimental studies have shown that the compositions of amphiboles are not strongly influenced by changes in the coexisting crystalline assemblage (Helz, 1982).

Amphibole and phlogopite were chosen for study because of the many chemical substitutions permissible within these minerals that might help elucidate the last stages of crystallization; in addition, these minerals could give information on the possible role of fluids in postcumulus processes in layered mafic stratiform intrusions. In particular, the Al^{IV} and Ti contents of amphiboles are strongly correlated with temperature (Helz, 1973). Furthermore, the Cl and F contents of the amphiboles should give evidence for the presence of these volatiles in the original melt (Wones and Gilbert, 1982).

This report documents the textural and chemical characteristics of postcumulus amphibole and phlogopite in part of a layered mafic intrusion, compares these results with the whole-rock trace-element data on the host rocks, and tests hypotheses for late-stage processes, such as (1) the role of a fluid phase (Bow and others, 1982) and (2) simple crystallization from trapped (interstitial) magma.

Acknowledgments

We are grateful to Anaconda Minerals Company for making the drill core available for study and for cooperating fully with this project. Discussions with geologists of the Anaconda Minerals Company were of great benefit, as were the critical reviews by Rosalind Helz and Bruce Lipin. Steven W. Novak helped modify the computer programs used in calculating the mineral formulas so as to include Cr_2O_3.

DISTRIBUTION, TEXTURE, AND MICROSCOPIC RELATIONS OF AMPHIBOLE AND PHLOGOPITE

Mineralogy and Petrology of the Olivine Cumulate

The cyclic unit investigated in this study was intersected in a diamond-drill hole in the upper part of Nye Basin, east of the Stillwater River. The stratigraphic position of this section in the lower part of the Ultramafic series and the correlation of the section with measured sections elsewhere in the complex are reported by Jackson (1968) and Page and others (1972). The samples used in this study are from the olivine cumulate at the base of this cyclic unit. Most of the mineralogic, petrologic, and geochemical information on the cumulus minerals incorporated in this report are from Page and others (1972).

Olivine grain-size measurements, olivine compositions, and volume percentages of postcumulus material are shown in figure 1 as a framework for discussing the distribution of amphibole and phlogopite. The cumulates can be subdivided into a series of nine subunits based upon the grain size of olivine and the abundance of chromite. In the first three subunits (fig. 1), the grain size of olivine decreases systematically within each subunit. Subunits 4 and 5 contain chromite, olivine-chromite, and olivine cumulates and are thus distinct. Subunits 7, 8, and 9 are largely based on olivine grain size, which decreases in each subunit; however, the lower 80 percent of subunit 9 contains no cumulus spinel phase, in contrast to all of the other subunits, which contain cumulus chromite in minor amounts. Variations in volume percentages of minerals, in mineral compositions, and in trace-element contents correlate with size-graded subunits of the olivine cumulate (Page and others, 1972).

The olivine cumulate of this cyclic unit is fairly typical for the Ultramafic series and on the average contains 70.9 volume percent cumulus olivine, with an average $Mg/(Mg + Fe^{2+}) \times 100 = 84.0$. In addition, the average total mode contains 1.7 percent cumulus chromite and traces of pyrrhotite, pentlandite, and chalcopyrite both as inclusions in cumulus grains and as postcumulus grains. Postcumulus plagioclase (11.1 percent), orthopyroxene (6.0 percent), augite (9.0 percent), hornblende (0.7 percent), and phlogopite (0.5 percent) account for the rest of the unserpentinized rock. Serpentinization and postcrystallization alteration have produced various amounts of the alteration assemblage lizardite + chrysotile $\pm$ magnetite $\pm$ thompsonite (or other zeolites) $\pm$ calcite, the details of which are discussed in Page (1976).

Variation in Amount of Amphibole and Phlogopite in the Olivine Cumulate

Within the olivine cumulate, the maximum amounts of combined amphibole and phlogopite are found in size-graded subunits 3, 4, and 5 (fig. 1*D*). These are the subunits immediately below and containing the chromite and olivine-chromite cumulate layers. There are no overall systematic trends in the abundance of combined amphibole and phlogopite with stratigraphic height within the entire section. However, the combined abundance of amphibole and phlogopite decreases upsection within subunit 3, which is the subunit below the first chromite cumulates.

Either phlogopite or amphibole may be the more abundant mineral in any particular sample (fig. 1*D*); however, no recognizable patterns to their relative abundance were found. Also, there are no stratigraphic patterns to their mode of textural occurrence.

Microscopic Textures and Associations

Amphibole and phlogopite are not randomly distributed within a thin section but instead show very subtle but consistent textural relations with other postcumulus and cumulus minerals. Two generations of amphibole are present: (1)

brown to red-brown (β), brown to light-brown (γ), and colorless (α) crystals that texturally appear to be part of the postcumulus magmatic assemblage; and (2) colorless crystals that appear to be the product of a subsolidus alteration event. The terms brown amphibole and hornblende are used interchangeably to describe amphiboles of generation (1). Phlogopite is the only mica recognized; it forms brownish-red (β and γ) and pale-yellow (α) crystals that also appear to be part of the postcumulus magmatic assemblage.

Commonly, postcumulus brown amphibole is spatially associated with either postcumulus pyroxene, cumulus chromite, or both. The association with pyroxene may be direct, in which case brown amphibole forms discontinuous rims on augite (fig. 2*A*) or, less commonly, on orthopyroxene (fig. 2*B*). The textures of these rims indicate that the hornblende is replacing the pyroxene. Features suggesting replacement include (1) irregular grain boundaries between hornblende and pyroxene, (2) optically continuous patches

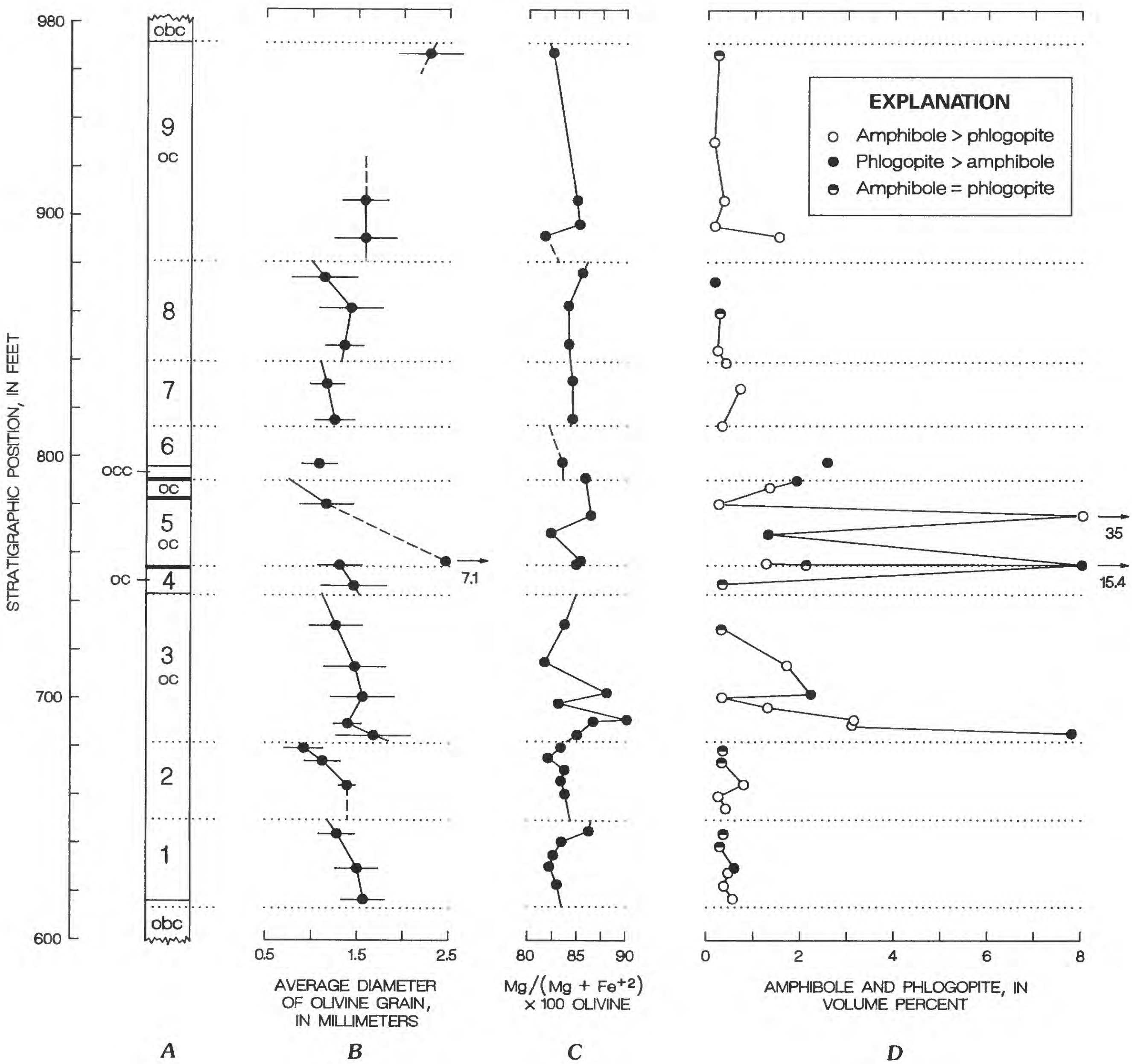

Figure 1. Combined modal volume of amphibole and phlogopite correlated with stratigraphic position in cyclic unit 2. *A*, Columnar section of cyclic unit 2 showing subunits 1 through 9 (dotted lines), upper part of Nye Basin; oc, olivine cumulate; obc,olivine-bronzite cumulate; occ, olivine-chromite cumulate; heavy lines, chromite cumulate. Scale is in drilling footage. *B*, Size of olivine as average diameter. Horizontal lines are error bars. Dashed lines indicate values extend off scale. Actual value is shown by arrow. *C*, Olivine compositions as determined by X-ray diffraction. *D*, Combined volume percentage of amphiboles and phlogopite.

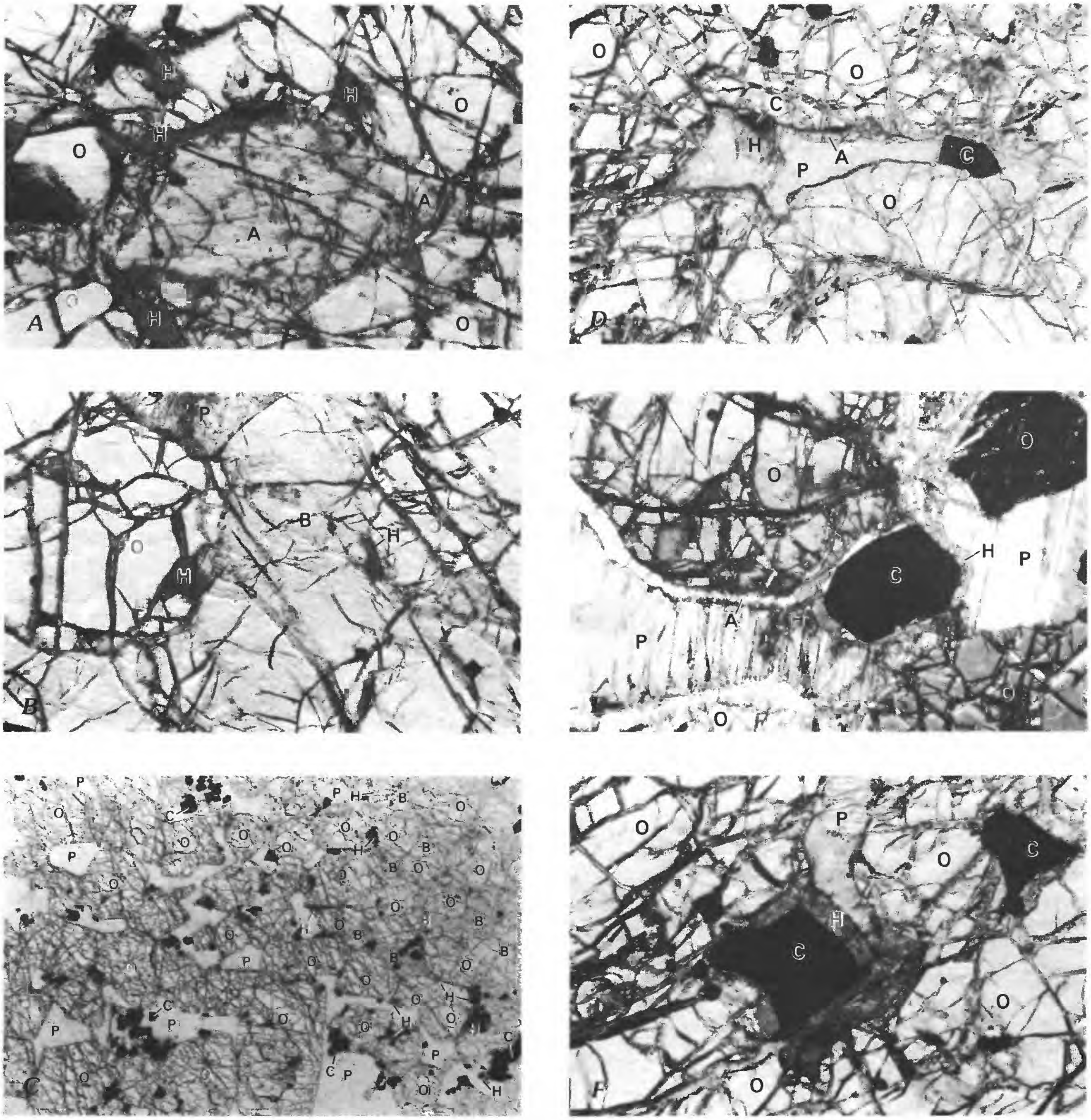

Figure 2. Photomicrographs showing textures of primary brown amphibole and phlogopite in olivine cumulates from cyclic unit 2 of the Periodotite zone of the Ultramafic series, Nye Basin area. Long dimension of all photomicrographs is 2.4 mm except as noted. All samples were photographed in plane-polarized light except as noted. O, olivine; B, orthopyroxene; A, augite; P, plagioclase; C, chromite; H, hornblende; ph, phlogopite. *A*, Brown amphibole rim on postcumulus augite. Sample NB9 691.5. *B*, Brown amphibole rim on postcumulus orthopyroxene. Sample NB9 665. *C*, Thin section of entire slide, showing brown amphibole adjacent to oikocryst. Long dimension of photograph is 10 mm. *D*, Brown amphibole rim on cumulus chromite that is continuous with a clinopyroxene rim on olivine. Sample NB9 630. *E*, Brown amphibole rim on cumulus chromite that is continuous with a clinopyroxene rim on olivine. Sample NB9 715. *F*, Brown amphibole rim on cumulus chromite. Sample NB9 618. *G*, Brown amphibole rim on cumulus chromite. Sample NB9 830a. *H*, Subhedral phlogopite associated with cumulus chromite and postcumulus plagioclase. Sample NB9 628. *I*, Coexisting phlogopite and brown amphibole. Sample NB9 715. *J*, Coexisting phlogopite and brown amphibole. Sample NB9 755b.

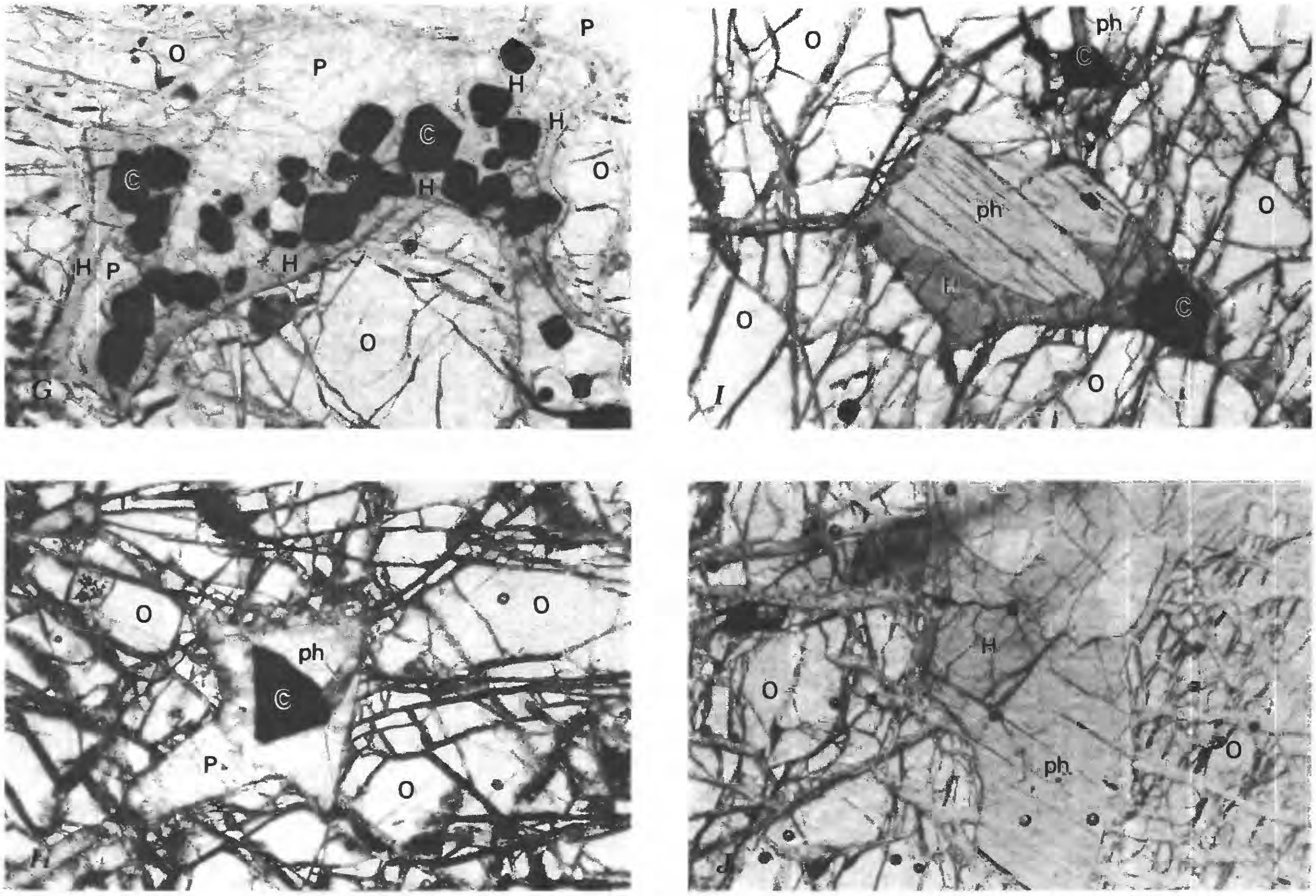

Figure 2. Continued.

and lenses of hornblende within the cores of pyroxene crystals, and (3) examples of twinned hornblende crystals that are homoaxial with twinned augite crystals. On a larger scale, the distribution of hornblende in a thin section may be spatially related to pyroxene even though hornblende does not directly form rims on the pyroxene. As an example, postcumulus hornblende is concentrated in a zone adjacent to an orthopyroxene oikocryst (fig. 2*C*).

The association between chromite and brown amphibole is much more direct (fig. 2*D*, *E*). In these examples, thin rims of augite have formed between cumulus olivine and interstitial plagioclase. However, where similar rims form on cumulus chromite, the rim material is brown amphibole. In most cases, however, brown amphibole forms rims adjacent to chromite without any associated augite (fig. 2*F*, *G*). Rims of hornblende between cumulus olivine grains or between cumulus olivine and interstitial plagioclase are common; however, some of these occurrences may be related to the other textural occurrences outside the plane of the thin section.

Clear, colorless amphibole is quite rare in these rocks, having been observed in only two samples. The clear amphibole may rim and replace brown amphibole, but it also replaces pyroxene. In some examples, the hornblende crystals are altered to the clear, colorless amphibole through various brown color zones. This alteration may be associated with serpentinization, as described by Page (1976).

Postcumulus phlogopite forms subhedral to euhedral books when it is finer grained, but it may form anhedral irregular grains where it completely fills the interstitial void between cumulus grains. Phlogopite may preferentially form subhedral crystals growing adjacent to chromite grains (fig. 2*H*) or rims on opaques, but it does not tend to be associated with postcumulus pyroxene, unlike brown amphibole.

Coexisting brown amphibole and phlogopite was not commonly observed, and only three examples of it were found in this study. Boundaries between these minerals do not yield any information on the relative order of crystallization (fig. 2*I*, *J*). Instead, the boundaries between brown amphibole and biotite appear to represent minimum free-energy grain-boundary configurations for these two minerals (Kretz, 1966).

The idiomorphic grain boundaries exhibited by phlogopite in contact with plagioclase suggest that the mica crystallized prior to or contemporaneously with plagioclase. The relative order of plagioclase and brown amphibole crystallization is more difficult to gauge. Because brown amphibole does not develop idiomorphic grain boundaries against plagioclase, it is assumed to have crystallized contemporaneously with or subsequent to plagioclase.

TECHNIQUES

The methods of handling and gathering data from the drill core, in addition to the whole-rock trace-element analyses for the rocks studied, are described by Page and others (1972). The mineral presented in this report are microprobe analyses collected at facilities at the U.S. Geological Survey in Menlo Park, California, and the University of California, Berkeley. The amphibole and phlogopite analyses reported in the present study are of either single points on mineral grains or an average of several points on the same crystal. The points on the mineral grains (reported in the tables as, for example, 618a-pt 1) were selected to be representative of a given textural occurrence and to be free of any alteration or grain-boundary interference. Multiple analyses were made on the larger grains; commonly, these analyses were in the core of the crystal and along its rim. If a difference in composition was present, the individual analyses are reported. However, if they were similar, the average composition of the multiple points is presented.

The analyses of brown amphibole, secondary amphibole, and phlogopite conducted at the U.S. Geological Survey at Menlo Park were performed on an automated three-channel ARL-EMX electron microprobe. Point locations were recorded on photomicrographs to assist in relocation. Each element was determined by wavelength dispersive analysis. Standard operating conditions were an accelerating potential of 15 kV with a sample current of approximately 0.03 μA. For each point analysis, the counts for each element represent the average of six separate counting intervals. The length of the counting interval was approximately 10 s and was determined by beam-current integration. The information was collected, stored on-line, and reduced with the program FRAME 64 using the procedure outlined in Yakowitz and others (1973).

Analyses of the zoned brown amphiboles, olivines, and chromites were performed on an eight-channel ARL-SEMQ microprobe at the University of California, Berkeley. The elements were determined by wavelength dispersive analysis; operating conditions were identical to those for the analyses done at Menlo Park. Each point analysis of amphibole represents the average of six 10-s fixed-beam counting intervals. The analyses of olivine and chromite represent averages of analyses of multiple points within a crystal. The information was collected and reduced on-line using the program PRMAIN developed by M. Rivers.

The accuracy and precision can be estimated because amphibole and biotite standards periodically were analyzed as unknown minerals. When compared with the reported values of the standard, the average analyses of the standards that were analyzed as unknowns provide an estimate of the accuracy of the analyses (table 1). Because of the small variations in composition discussed in this report, the data in table 1 are provided to aid the reader in evaluating the analyses presented. The standard deviations demonstrate the level of precision and hence the analytical error typical of analyses collected on the ARL-EMX microprobe. The precision of analyses collected on the ARL-SEMQ microprobe is comparable to or slightly better than that of the ARL-EMX microprobe analyses.

All mineral formulas are reported to three decimal places and were calculated before rounding the analytical data to minimize rounding errors, but they are probably not significant to more than two places. Mineral formulas of amphiboles were calculated on the basis of 23 oxygens using the program described by Papike and others (1974). The Fe^{3+} values reported for the analyses are the minimum values calculated by this program. Mineral formulas for phlogopites were calculated using an unpublished program developed by S. Ludington. The mineral formulas for phlogopites are based on the assumption that the sum of the positive charges equals 22. Olivine and chromite mineral formulas were calculated on the basis of 4 oxygens. Estimates of Fe_2O_3 in the chromites are based on stoichiometry.

COMPOSITION AND SUBSTITUTION MECHANISMS OF AMPHIBOLE

The chemical compositions and calculated mineral formulas of primary brown hornblendes and secondary colorless amphiboles are given in tables 2 and 3, respectively. This section outlines the compositional limits of the amphiboles analyzed in this study.

The general form of the standard amphibole formula is $A_{0-1}\ B_2\ C_5^{VI}\ T_8^{IV}\ O_{22}\ (OH, F, Cl)_2$, where T represents tetrahedral sites occupied by Si and Al; C represents the M_1, M_2, and M_3 octahedral sites, which are commonly occupied by Al, Cr, Ti, Fe, Mg, and Mn; B represents the 6- to 8-coordinated M_4 site occupied by Fe, Mn, Mg, Ca, and Na; and A represents the 10- to 12-coordinated A site, which may be occupied by Na and K (Leake, 1978).

The brown amphiboles are calcic, with $(Ca + Na)_B \geqslant 1.34$ and $Na_B < 0.67$. In addition, these amphiboles have $Ti < 0.50$ and calculated $Fe^{3+} < Al^{VI}$. These amphiboles are classified as pargasite or pargasitic hornblende (fig. 3*A*).

The alteration amphiboles are also calcic and are classified as pargasite, pargasitic hornblende, edenitic hornblende, and magnesio-hastingsitic hornblende (transitional

Table 1. Electron microprobe analyses of standard amphibole and biotite compared with reported analyses of the standards
[n.d., not determined]

	1	2	3		4	5	6
SiO_2 ------	40.50	0.26	40.54	SiO_2---	39.07	0.80	38.63
Al_2O_3 -----	10.14	.22	10.10	Al_2O_3--	13.17	.22	13.10
FeO -------	26.25	.30	26.28	TiO_2---	1.68	.04	1.58
MgO -------	4.35	.10	4.37	FeO----	11.18	.18	10.92
TiO_2 ------	2.84	.24	2.88	MgO----	19.79	.10	19.90
CaO -------	10.46	.15	10.49	Cr_2O_3--	.18	.07	.23
Na_2O ------	1.95	.11	2.24	CaO---	.01	.02	.00
K_2O -------	1.48	.04	1.45	Na_2O---	.32	.04	.15
Cr_2O_3 -----	.01	.01	n.d.	K_2O----	10.00	.04	10.00
Cl --------	.16	.03	.18	F------	.13	.01	.30
F ---------	.18	.02	.27	Cl-----	.01	.00	n.d.
Total---	98.32	—	98.80	Total-	95.54	—	94.81
Formula based on 23 oxygens				Formula based on sum of positive charges=22			
Si --------	6.393	.038	6.382	Si-----	2.873	.027	2.866
Al^{IV} ------	1.607	.038	1.618	Al^{IV}---	1.173	.097	1.134
ΣTet ------	8.000		8.000	Al^{IV}---	.018	.023	.012
Al^{VI} ------	.284	.033	.256	Ti-----	.093	.003	.088
Fe --------	3.465	.048	3.460	Fe^{2+}---	.686	.017	.678
Mg --------	1.025	.022	1.025	Mg-----	2.170	.033	2.201
Ti --------	.336	.026	.341	Cr-----	.006	.002	.007
Cr --------	.001	.002	.000	ΣOct---	2.974	.025	2.985
ΣOct ------	5.111	.025	5.082	Ca-----	.001	.001	.000
Excess Oct-	.111	.025	.082	Na-----	.046	.005	.022
Ca --------	1.770	.018	1.769	K------	.937	.010	.947
Na_B -------	.119	.027	.149	F------	.030	.004	.070
ΣB --------	2.000		2.000	Cl-----	.001	.000	n.d.
Na_A -------	.478	.031	.535	OH-----	1.969	.004	n.d.
K ---------	.299	.009	.291	Xmg----	.73	.01	.74
ΣA site ---	.777	.029	.826	Xph----	.73	.01	.74
$Mg/(Mg+Fe^{2+})$	.23	.01	.23	Xan----	.20	.01	.19
				Xsid---	.08	.01	.07

1. Average of 12 Amp 52 analyses that were run as unknowns.
2. Standard deviations on the average reported in column 1.
3. Reported analysis of Amp 52.
4. Average of four Bio 56 analyses that were run as unknowns.
5. Standard deviations on the average reported in column 4.
6. Reported analysis of Bio 56.

pale-brown crystals) to tremolite or tremolitic hornblende (colorless crystals).

Earlier, we described at least two distinctly different textural occurrences of hornblende. Hornblende was found both to replace augite (fig. 2*A*) and to form rims on chromite crystals (fig. 2*D–G*). To assess the role of assemblage on hornblende compositions, the analyses were sorted into the following categories: (1) hornblende that rims chromite but does not replace pyroxene, (2) hornblende that replaces augite but is not in contact with chromite, (3) hornblende occurring in the lower portion of subunit 9 in which a cumulus spinel phase is not present, and (4) hornblende in ambiguous or different textural associations (table 2).

The mean and standard deviation for each textural group were calculated, and the differences between the means of oxide weight percentage and formula units for the groups were tested at a 0.5-percent level by calculating a comparison criterion that is based on the pooled standard deviation, on Student's t-test, and on the number of samples in each group. This value is then compared with the absolute difference between the means of the property between groups that is under consideration. Means and standard deviations are presented in table 4, and the results of the comparison are given in table 5.

If the mean difference is greater than the comparison criterion reported in table 5, the means for that property

Table 2. Electron microprobe analyses and calculated mineral formulas of hornblendes from the olivine cumulate of cyclic unit 2, Stillwater Complex, Montana
[Analyst: M.L. Zientek. n.d., not determined]

	618a-pt 1	618b-pt 3	623a-pt 13	623b-pt 14	628b-pt 12	628c-pt 10	630b-pt 7	630b-pt 8
Microprobe analyses, weight percent								
SiO_2	42.6	42.8	44.2	43.5	43.3	43.7	43.2	43.6
Al_2O_3	12.0	12.1	12.0	11.6	12.0	11.8	11.7	12.2
FeO	6.0	5.7	5.7	6.4	6.2	6.3	5.5	5.8
MgO	16.6	16.4	15.7	16.0	15.8	15.7	15.8	15.6
TiO_2	3.0	1.6	2.9	2.7	2.5	2.7	3.3	3.2
CaO	11.5	11.6	11.6	11.9	11.7	11.9	12.1	11.6
Na_2O	2.4	2.4	2.3	2.4	2.2	2.3	2.3	2.3
K_2O	1.0	1.0	1.1	1.0	1.1	1.0	1.1	1.1
Cr_2O_3	1.1	1.6	1.4	1.3	1.5	1.5	1.4	1.4
Cl	.06	.08	.10	.12	.11	.12	.15	.03
F	.01	.05	.09	.10	.08	.08	.04	.15
Total	96.27	95.33	97.09	97.02	96.49	97.10	96.59	96.98
Mineral formula calculated on the basis of 23 oxygens								
Si	6.236	6.312	6.381	6.340	6.330	6.340	6.297	6.316
Al^{IV}	1.764	1.688	1.619	1.660	1.670	1.660	1.703	1.684
Σ Tet	8.000	8.000	8.000	8.000	8.000	8.000	8.000	8.000
Al^{VI}	.304	.417	.423	.337	.390	.365	.313	.402
Fe^{2+}	.709	.699	.693	.781	.762	.766	.670	.697
Fe^{3+}	.000	.000	.000	.000	.000	.000	.000	.000
Mg	3.621	3.608	3.380	3.461	3.445	3.405	3.421	3.372
Ti	.331	.181	.318	.290	.271	.289	.365	.351
Cr	.128	.190	.164	.146	.169	.169	.160	.158
Σ Oct	5.094	5.095	4.979	5.015	5.037	4.994	4.929	4.980
Excess Oct	.094	.095	.000	.015	.037	.000	.000	.000
Ca	1.808	1.830	1.792	1.855	1.827	1.857	1.895	1.799
Na_B	.098	.074	.208	.129	.135	.143	.105	.200
ΣB	2.000	2.000	2.000	2.000	2.000	2.000	2.000	2.000
Na_A	.572	.603	.437	.545	.499	.513	.544	.452
K	.194	.190	.208	.180	.205	.191	.204	.209
Σ A site	.766	.793	.645	.726	.704	.704	.749	.661
$Mg/(Mg+Fe^{2+})$	.84	.84	.83	.82	.82	.82	.84	.83
Accept[1]	Yes	Yes	No	Yes	Yes	Yes	No	No
Accept[2]	--	Yes	--	--	--	--	Yes	--
Name	Pargasite	Pargasitic hornblende	Pargasitic hornblende	Pargasitic hornblende	Pargasitic hornblende	Pargasitic hornblende	Pargasitic hornblende	Pargasitic hornblende
Assemblage[3]	4	1	1	4	2	1	1	1

	640a-1,2	640b-3,4	640c-1,2,3	640c-4,5	645a-1,2	645b-pt 2	645c-1,2	655b-pt 5	655-pt 6
Microprobe analyses, weight percent									
SiO_2	43.0	43.0	42.9	43.2	42.6	43.1	43.1	43.9	42.9
Al_2O_3	11.9	12.0	12.0	12.0	12.5	11.9	12.0	11.3	11.8
FeO	6.3	6.3	6.2	6.4	5.7	6.9	6.2	6.1	7.4
MgO	15.3	15.5	15.4	15.3	15.2	15.6	15.6	15.7	16.5
TiO_2	3.0	2.5	2.9	2.8	3.3	2.6	3.0	3.3	3.0
CaO	11.8	11.7	11.7	11.8	12.0	11.9	11.7	11.6	10.9
Na_2O	2.5	2.4	2.4	2.3	2.3	2.5	2.4	2.4	2.2
K_2O	.8	1.0	1.0	1.0	1.1	.9	1.1	.9	.8
Cr_2O_3	1.6	1.6	1.6	1.6	1.3	1.3	1.1	1.5	.9
Cl	n.d.	n.d.	n.d.	n.d.	n.d.	n.d.	n.d.	.13	.14
F	n.d.	n.d.	n.d.	n.d.	n.d.	n.d.	n.d.	.08	.08
Total	96.2	96.0	96.1	96.4	96.0	96.7	96.2	96.9	96.62
Mineral formula calculated on the basis of 23 oxygens									
Si	6.298	6.314	6.284	6.316	6.238	6.296	6.304	6.378	6.273
Al^{IV}	1.702	1.686	1.716	1.684	1.762	1.704	1.696	1.622	1.727
Σ Tet	8.000	8.000	8.000	8.000	8.000	8.000	8.000	8.000	8.000
Al^{VI}	.346	.388	.364	.381	.393	.343	.374	.317	.305
Fe^{2+}	.767	.776	.763	.784	.702	.848	.762	.743	.903
Fe^{3+}	.000	.000	.000	.000	.000	.000	.000	.000	.000
Mg	3.343	3.383	3.371	3.337	3.320	3.390	3.398	3.403	3.587
Ti	.334	.276	.317	.304	.367	.290	.328	.356	.330
Cr	.186	.185	.183	.187	.147	.150	.128	.169	.105
Σ Oct	4.976	5.007	4.998	4.994	4.929	5.021	4.990	4.988	5.230
Excess Oct	.000	.007	.000	.000	.000	.021	.000	.000	.230
Ca	1.847	1.840	1.836	1.839	1.880	1.862	1.839	1.801	1.715
Na_B	.152	.152	.163	.161	.120	.116	.161	.199	.055
ΣB	2.000	2.000	2.000	2.000	2.000	2.000	2.000	2.000	2.000
Na_A	.560	.528	.515	.502	.544	.581	.520	.485	.555
K	.142	.185	.187	.179	.206	.166	.198	.163	.157
Σ A site	.702	.713	.702	.681	.750	.747	.718	.648	.711
$Mg/(Mg+Fe^{2+})$	.81	.81	.82	.81	.83	.80	.82	.82	.80
Accept[1]	No	Yes	Yes	Yes	No	Yes	Yes	No	Yes
Accept[2]	Yes	--	--	--	--	--	--	Yes	--
Name	Pargasitic hornblende	Pargasitic hornblende	Pargasitic hornblende	Pargasitic hornblende	Pargasitic hornblende	Pargasitic hornblende	Pargasitic hornblende	Pargasitic hornblende	Pargasitic hornblende
Assemblage[3]	2	2	1	2	1	4	4	4	4

Table 2. Electron microprobe analyses and calculated mineral formulas of hornblendes from the olivine cumulate of cyclic unit 2, Stillwater Complex, Montana—*Continued*

	655a a-1,2	655a b-pt 2	657a-1,3	657b-1,2,3	660a-pt 2	660a-pt 3	660b-1,2	665a-1,2	665a-pt 3
				Microprobe analyses, weight percent					
SiO_2	42.5	42.2	42.5	42.9	42.9	42.6	42.8	42.2	42.1
Al_2O_3	12.2	11.8	12.1	11.9	12.1	12.0	12.4	12.5	13.1
FeO	5.8	6.1	6.0	6.1	6.4	5.9	5.9	6.2	6.4
MgO	15.6	15.9	15.9	15.9	15.7	15.7	15.6	15.3	15.9
TiO_2	3.2	3.2	2.9	2.8	3.1	3.3	3.1	3.0	3.0
CaO	11.8	11.7	11.6	11.7	11.7	11.7	11.6	11.6	11.6
Na_2O	2.4	2.6	2.5	2.5	2.6	2.6	2.4	2.4	2.3
K_2O	1.1	.9	1.0	1.0	1.0	.8	1.0	1.1	1.0
Cr_2O_3	1.4	1.4	1.2	1.4	1.5	1.5	1.5	1.5	1.4
Cl	n.d.	n.d.	n.d.	n.d.	n.d.	n.d.	n.d.	n.d.	n.d.
F	n.d.	n.d.	n.d.	n.d.	n.d.	n.d.	n.d.	n.d.	n.d.
Total	96.0	96.5	95.7	96.2	97.0	96.1	96.3	95.8	96.8
				Mineral formula calculated on the basis of 23 oxygens					
Si	6.229	6.213	6.257	6.277	6.250	6.240	6.247	6.221	6.136
Al^{IV}	1.771	1.786	1.743	1.723	1.749	1.760	1.752	1.779	1.864
Σ Tet	8.000	8.000	8.000	8.000	8.000	8.000	8.000	8.000	8.000
Al^{VI}	.338	.270	.356	.335	.322	.308	.380	.388	.393
Fe^{2+}	.716	.754	.740	.748	.779	.718	.723	.763	.784
Fe^{3+}	.000	.000	.000	.000	.000	.000	.000	.000	.000
Mg	3.409	3.487	3.479	3.475	3.404	3.430	3.393	3.362	3.443
Ti	.351	.352	.316	.307	.334	.365	.338	.330	.326
Cr	.162	.167	.141	.164	.167	.173	.172	.169	.157
Σ Oct	4.976	5.030	5.033	5.030	5.007	4.993	5.008	5.011	5.102
Excess Oct	.000	.030	.033	.030	.007	.000	.008	.011	.102
Ca	1.859	1.841	1.823	1.830	1.831	1.834	1.823	1.826	1.813
Na_B	.141	.129	.144	.139	.162	.166	.169	.162	.085
ΣB	2.000	2.000	2.000	2.000	2.000	2.000	2.000	2.000	2.000
Na_A	.549	.608	.566	.567	.576	.584	.513	.524	.562
K	.207	.165	.191	.181	.177	.146	.179	.201	.186
Σ A site	.757	.774	.757	.748	.753	.730	.692	.726	.748
$Mg/(Mg+Fe^{2+})$	.83	.82	.82	.82	.81	.83	.82	.82	.81
Accept[1]	No	Yes	Yes	Yes	Yes	Yes	Yes	Yes	Yes
Accept[2]	Yes	--	--	--	--	--	--	--	--
Name	Pargasite	Pargasite	Pargasitic hornblende	Pargasitic hornblende	Pargasitic hornblende	Pargasite	Pargasite	Pargasite	Pargasite
Assemblage[3]	1	4	4	4	1	4	2	1	4

	665b-1,2	675a-pt 1	675a-2,3	675b-1,2	680a-pt 1	680a-pt 2	690a-1,3,4	690b-1,2	690c-1,2
				Microprobe analyses, weight percent					
SiO_2	42.5	42.8	43.1	42.9	43.2	43.1	42.9	42.9	42.4
Al_2O_3	12.0	12.5	12.0	12.1	12.2	11.9	12.1	11.8	12.1
FeO	6.1	5.8	6.0	5.9	5.6	5.8	6.2	6.4	5.8
MgO	15.2	15.6	15.6	15.5	15.7	15.6	15.5	15.4	15.5
TiO_2	3.3	2.9	3.0	3.5	2.4	3.1	2.3	2.5	3.0
CaO	11.6	11.9	11.6	11.8	12.1	11.8	11.7	11.8	11.7
Na_2O	2.6	2.4	2.4	2.4	2.4	2.4	2.3	2.2	2.4
K_2O	.8	1.1	1.0	.8	1.0	1.0	1.0	1.0	1.0
Cr_2O_3	1.5	1.4	1.3	1.5	1.2	1.5	1.4	1.5	1.4
Cl	n.d.	n.d.	n.d.	n.d.	n.d.	n.d.	n.d.	n.d.	n.d.
F	n.d.	n.d.	n.d.	n.d.	n.d.	n.d.	n.d.	n.d.	n.d.
Total	95.6	96.4	96.0	96.4	95.8	96.1	95.4	95.5	95.3
				Mineral formula calculated on the basis of 23 oxygens					
Si	6.267	6.249	6.300	6.259	6.324	6.301	6.323	6.320	6.262
Al^{IV}	1.733	1.751	1.700	1.741	1.676	1.699	1.677	1.680	1.738
Σ Tet	8.000	8.000	8.000	8.000	8.000	8.000	8.000	8.000	8.000
Al^{VI}	.351	.392	.375	.338	.438	.352	.428	.372	.367
Fe^{2+}	.750	.707	.732	.721	.687	.707	.768	.783	.713
Fe^{3+}	.000	.000	.000	.000	.000	.000	.000	.000	.000
Mg	3.335	3.399	3.398	3.363	3.428	3.400	3.412	3.392	3.417
Ti	.361	.323	.332	.379	.263	.338	.256	.277	.331
Cr	.176	.159	.155	.174	.142	.169	.161	.179	.162
Σ Oct	4.974	4.980	4.992	4.976	4.960	4.966	5.025	5.003	4.990
Excess Oct	.000	.000	.000	.000	.000	.000	.025	.003	.000
Ca	1.828	1.861	1.825	1.841	1.895	1.854	1.849	1.867	1.854
Na_B	.172	.139	.175	.159	.105	.146	.126	.130	.145
ΣB	2.000	2.000	2.000	2.000	2.000	2.000	2.000	2.000	2.000
Na_A	.562	.537	.506	.526	.565	.534	.519	.510	.530
K	.145	.195	.190	.153	.187	.183	.184	.194	.183
Σ A site	.707	.732	.696	.679	.752	.717	.703	.704	.712
$Mg/(Mg+Fe^{2+})$	.82	.83	.82	.82	.83	.83	.82	.81	.83
Accept[1]	No	No	Yes	No	No	No	Yes	Yes	Yes
Accept[2]	Yes	Yes	--	Yes	--	--	--	--	--
Name	Pargasitic hornblende	Pargasite	Pargasitic hornblende	Pargasitic hornblende	Pargasitic hornblende	Pargasitic hornblende	Pargasitic hornblende	Pargasitic hornblende	Pargasitic hornblende
Assemblage[3]	4	1	4	1	2	1	4	2	1

Table 2. Electron microprobe analyses and calculated mineral formulas of hornblendes from the olivine cumulate of cyclic unit 2, Stillwater Complex, Montana—*Continued*

	690c-pt 3	691.5a-3,4	691.5b-1,2	697.5a-pt 6	697.5b-4,5	701b-pt 7	715a-8,9	715b-pt 10	715b-pt 11
Microprobe analyses, weight percent									
SiO_2	42.8	43.4	44.1	42.9	42.6	42.7	42.4	42.2	42.7
Al_2O_3	11.8	11.1	11.3	11.9	11.4	11.6	11.9	11.4	12.1
FeO	6.2	6.4	6.3	6.3	6.0	6.1	6.1	5.7	6.3
MgO	15.4	15.8	15.9	16.5	16.4	16.3	16.0	16.1	16.5
TiO_2	2.9	3.6	3.4	2.8	3.5	2.9	3.1	3.6	2.4
CaO	12.0	11.7	12.0	11.2	11.3	11.3	11.2	10.3	11.3
Na_2O	2.4	2.4	2.5	2.5	2.5	2.6	2.4	2.3	2.3
K_2O	.9	.8	.7	.8	.6	.6	1.0	1.2	1.1
Cr_2O_3	1.6	1.4	1.5	1.2	1.5	1.5	1.6	1.6	1.4
Cl	n.d.	.17	.15	.18	.11	.22	.30	.10	.12
F	n.d.	.07	.09	.06	.06	.03	.05	.02	.06
Total	96.0	96.84	97.94	96.34	95.97	95.85	96.5	94.52	96.28
Mineral formula calculated on the basis of 23 oxygens									
Si	6.303	6.335	6.357	6.280	6.254	6.279	6.239	6.281	6.259
Al^{IV}	1.697	1.665	1.643	1.720	1.746	1.721	1.761	1.718	1.741
Σ Tet	8.000	8.000	8.000	8.000	8.000	8.000	8.000	8.000	8.000
Al^{VI}	.355	.244	.274	.334	.221	.283	.298	.283	.347
Fe^{2+}	.767	.776	.760	.765	.735	.747	.745	.714	.774
Fe^{3+}	.000	.000	.000	.000	.000	.000	.000	.000	.000
Mg	3.391	3.436	3.411	3.590	3.583	3.569	3.516	3.568	3.607
Ti	.318	.390	.366	.308	.384	.319	.346	.400	.267
Cr	.181	.156	.165	.142	.175	.174	.186	.185	.162
Σ Oct	5.012	5.002	4.976	5.140	5.099	5.092	5.092	5.150	5.157
Excess Oct	.012	.002	.000	.140	.099	.092	.092	.150	.157
Ca	1.830	1.825	1.848	1.752	1.778	1.788	1.768	1.636	1.766
Na_B	.158	.173	.152	.108	.122	.119	.141	.213	.077
ΣB	2.000	2.000	2.000	2.000	2.000	2.000	2.000	2.000	2.000
Na_A	.513	.511	.541	.588	.587	.629	.533	.444	.573
K	.169	.147	.129	.148	.116	.116	.191	.220	.204
Σ A site	.683	.658	.670	.736	.703	.745	.724	.665	.777
$Mg/(Mg+Fe^{2+})$	.82	.82	.82	.82	.83	.83	.83	.83	.82
Accept[1]	Yes	Yes	No	Yes	Yes	Yes	Yes	Yes	Yes
Accept[2]	--	--	Yes	--	--	--	--	--	--
Name	Pargasitic hornblende	Pargasitic hornblende	Pargasitic hornblende	Pargasitic hornblende	Pargasitic hornblende	Pargasitic hornblende	Pargasite	Pargasitic hornblende	Pargasitic hornblende
Assemblage[3]	1	2	2	2	2	2	4	1	2

	730a-pt 1	730a-pt 2	730a-pt 3	730c-1,2	747b-pt 1	747b-2,3,4,5	747c-1,2	747c-pt 4	755a-12,13,14
Microprobe analyses, weight percent									
SiO_2	42.3	42.6	42.6	42.7	43.2	42.5	42.4	43.2	42.2
Al_2O_3	12.1	12.1	11.5	12.3	12.5	12.4	12.4	12.3	11.1
FeO	5.9	5.8	7.5	5.8	5.9	5.6	6.0	5.9	6.2
MgO	15.4	15.2	16.1	15.0	15.9	15.6	16.4	18.7	16.3
TiO_2	2.7	3.4	2.9	3.3	2.6	3.5	3.9	3.2	4.5
CaO	11.6	11.9	11.7	11.8	12.0	12.0	11.9	11.9	10.9
Na_2O	2.5	2.3	2.4	2.3	2.4	2.6	2.4	2.3	2.4
K_2O	1.0	1.1	.8	1.0	.9	1.0	1.1	.7	1.1
Cr_2O_3	1.4	1.4	1.2	1.0	.9	1.4	1.2	1.5	.7
Cl	n.d.	n.d.	n.d.	n.d.	n.d.	n.d.	n.d.	n.d.	.16
F	n.d.	n.d.	n.d.	n.d.	n.d.	n.d.	n.d.	n.d.	.08
Total	94.9	95.8	96.7	95.2	96.3	96.6	97.7	99.7	95.64
Mineral formula calculated on the basis of 23 oxygens									
Si	6.276	6.265	6.235	6.291	6.302	6.199	6.127	6.058	6.231
Al^{IV}	1.724	1.735	1.765	1.709	1.698	1.801	1.873	1.942	1.769
Σ Tet	8.000	8.000	8.000	8.000	8.000	8.000	8.000	8.000	8.000
Al^{VI}	.383	.356	.216	.432	.443	.328	.240	.101	.160
Fe^{2+}	.737	.710	.924	.714	.720	.684	.723	.453	.761
Fe^{3+}	.000	.000	.000	.000	.000	.000	.000	.243	.000
Mg	3.408	3.330	3.524	3.300	3.452	3.393	3.523	3.905	3.580
Ti	.301	.372	.318	.361	.285	.381	.422	.337	.500
Cr	.165	.165	.142	.118	.099	.157	.139	.167	.086
Σ Oct	4.994	4.934	5.125	4.925	4.999	4.943	5.047	5.205	5.087
Excess Oct	.000	.000	.125	.000	.000	.000	.047	.205	.087
Ca	1.843	1.872	1.838	1.870	1.874	1.878	1.841	1.795	1.729
Na_B	.157	.128	.036	.130	.126	.122	.112	.000	.183
ΣB	2.000	2.000	2.000	2.000	2.000	2.000	2.000	2.000	2.000
Na_A	.548	.523	.657	.531	.544	.603	.563	.626	.507
K	.195	.205	.149	.184	.169	.188	.199	.131	.200
Σ A site	.743	.728	.806	.715	.714	.791	.762	.757	.706
$Mg/(Mg+Fe^{2+})$	.82	.82	.79	.82	.83	.83	.83	.90	.82
Accept[1]	Yes	No	Yes	No	Yes	No	Yes	Yes	Yes
Accept[2]	--	--	--	--	--	--	--	--	--
Name	Pargasitic hornblende	Pargasitic hornblende	Pargasite	Pargasitic hornblende	Pargasitic hornblende	Pargasite	Pargasite	Magnesio-hastingsite	Pargasite
Assemblage[3]	4	1	1	4	4	1	1	1	2

Table 2. Electron microprobe analyses and calculated mineral formulas of hornblendes from the olivine cumulate of cyclic unit 2, Stillwater Complex, Montana—*Continued*

	755ba-1,2,3,4	755-bc	755ca-1,2,3	755ca-pt 4	755cb-pt 1	755cb-2,3	767a-1,3	780a-pt 2	780a-3,4
				Microprobe analyses, weight percent					
SiO_2	43.0	43.1	43.6	43.4	43.6	43.5	43.4	43.6	43.8
Al_2O_3	11.5	12.0	11.8	11.6	11.5	11.6	12.4	11.8	12.8
FeO	6.5	6.5	5.8	5.8	6.0	5.8	5.1	6.1	5.4
MgO	16.0	16.0	16.2	16.0	16.2	16.1	16.6	17.2	16.7
TiO_2	2.6	2.9	3.2	4.1	3.2	3.4	2.7	2.4	2.1
CaO	11.8	11.6	11.8	11.7	11.7	11.8	12.0	11.7	12.0
Na_2O	2.8	2.6	2.6	2.7	2.6	2.7	2.3	2.3	2.3
K_2O	.5	.8	.7	.7	.8	.7	.9	.6	.6
Cr_2O_3	1.2	2.9	1.4	1.2	1.4	1.6	1.4	1.2	1.2
Cl	n.d.	n.d.	n.d.	n.d.	n.d.	n.d.	n.d.	n.d.	n.d.
F	n.d.	n.d.	n.d.	n.d.	n.d.	n.d.	n.d.	n.d.	n.d.
Total	95.9	98.4	97.1	97.2	97.0	97.2	96.8	96.9	96.9
				Mineral formula calculated on the basis of 23 oxygens					
Si	6.317	6.205	6.305	6.279	6.317	6.293	6.276	6.308	6.307
Al^{IV}	1.683	1.795	1.695	1.721	1.683	1.707	1.724	1.692	1.693
Σ Tet	8.000	8.000	8.000	8.000	8.000	8.000	8.000	8.000	8.000
Al^{VI}	.309	.234	.324	.251	.279	.269	.392	.320	.486
Fe^{2+}	.800	.787	.703	.700	.727	.698	.618	.734	.649
Fe^{3+}	.000	.000	.000	.000	.000	.000	.000	.000	.000
Mg	3.503	3.426	3.490	3.445	3.506	3.469	3.567	3.706	3.588
Ti	.285	.311	.343	.441	.349	.370	.294	.261	.224
Cr	.139	.327	.154	.138	.160	.178	.160	.137	.136
Σ Oct	5.037	5.085	5.014	4.976	5.021	4.984	5.031	5.158	5.082
Excess Oct	.037	.085	.014	.000	.021	.000	.031	.158	.082
Ca	1.858	1.790	1.823	1.811	1.811	1.835	1.855	1.815	1.854
Na_B	.105	.125	.163	.189	.167	.165	.114	.027	.064
ΣB	2.000	2.000	2.000	2.000	2.000	2.000	2.000	2.000	2.000
Na_A	.678	.590	.558	.562	.574	.581	.525	.624	.573
K	.092	.147	.137	.124	.139	.135	.171	.116	.114
Σ A site	.769	.737	.694	.686	.713	.167	.696	.740	.687
$Mg/(Mg+Fe^{2+})$	.81	.81	.83	.83	.83	.83	.85	.83	.85
Accept[1]	Yes	Yes	Yes	No	Yes	No	Yes	Yes	Yes
Accept[2]	--	--	--	Yes	--	Yes	--	--	--
Name	Pargasitic hornblende	Pargasite	Pargasitic hornblende	Pargasitic hornblende	Pargasitic hornblende	Pargasitic hornblende	Pargasitic hornblende	Pargasitic hornblende	Pargasitic hornblende
Assemblage[3]	4	4	1	1	4	1	1	4	1

	787c-pt 9	787a-pt 10	787a-pt 11	830a-12,13,14	845a-1,2,3	845b-1,3	861a-1,2,3	890-b pt 2
				Microprobe analyses, weight percent				
SiO_2	42.3	42.5	42.0	42.1	43.0	43.0	42.6	42.8
Al_2O_3	11.7	11.6	12.2	11.9	12.4	12.1	12.3	12.3
FeO	5.7	5.5	5.3	5.9	6.1	5.9	5.6	7.4
MgO	17.3	17.2	17.0	17.2	16.3	16.3	15.8	17.1
TiO_2	3.2	3.4	3.6	3.1	2.5	2.8	3.6	2.0
CaO	11.5	11.4	11.5	11.4	11.9	12.0	11.9	11.2
Na_2O	2.4	2.5	2.5	2.4	2.4	2.4	2.3	2.3
K_2O	1.0	.9	1.0	1.0	1.1	1.0	1.1	.8
Cr_2O_3	1.7	1.8	1.6	1.6	1.2	1.5	1.3	.9
Cl	.08	.09	.08	.11	n.d.	n.d.	n.d.	.07
F	.06	.08	.09	.03	n.d.	n.d.	n.d.	.01
Total	96.94	96.97	96.87	96.74	96.9	97.0	96.5	96.88
				Mineral formula calculated on the basis of 23 oxygens				
Si	6.164	6.185	6.109	6.150	6.249	6.249	6.211	6.225
Al^{IV}	1.836	1.815	1.891	1.850	1.751	1.751	1.789	1.775
Σ Tet	8.000	8.000	8.000	8.000	8.000	8.000	8.000	8.000
Al^{VI}	.169	.168	.205	.198	.374	.321	.322	.337
Fe^{2+}	.689	.666	.650	.714	.744	.722	.680	.815
Fe^{3+}	.000	.000	.000	.000	.000	.000	.000	.084
Mg	3.755	3.717	3.684	3.743	3.527	3.518	3.430	3.697
Ti	.346	.375	.394	.335	.275	.305	.391	.223
Cr	.201	.203	.203	.188	.141	.170	.152	.105
Σ Oct	5.159	5.131	5.120	5.178	5.062	5.035	4.975	5.261
Excess Oct	.159	.131	.120	.178	.062	.035	.000	.261
Ca	1.793	1.778	1.793	1.787	1.847	1.860	1.859	1.739
Na_B	.048	.091	.087	.035	.091	.105	.141	.000
ΣB	2.000	2.000	2.000	2.000	2.000	2.000	2.000	2.000
Na_A	.643	.619	.615	.647	.573	.574	.511	.651
K	.180	.165	.182	.182	.204	.182	.212	.152
Σ A site	.823	.784	.797	.830	.777	.755	.723	.803
$Mg/(Mg+Fe^{2+})$	.84	.85	.85	.84	.83	.83	.83	.82
Accept[1]	Yes	Yes	Yes	Yes	Yes	Yes	No	Yes
Accept[2]	--	--	--	--	--	--	Yes	--
Name	Pargasite	Pargasite	Pargasite	Pargasite	Pargasite	Pargasite	Pargasite	Pargasite
Assemblage[3]	2	1	1	1	4	1	1	3

Table 2. Electron microprobe analyses and calculated mineral formulas of hornblendes from the olivine cumulate of cyclic unit 2, Stillwater Complex, Montana—*Continued*

	890a-4,5,6	894a-1,2,3	905a-1,2	930a-1,2,3	966-7,8
Microprobe analyses, weight percent					
SiO_2	43.9	43.5	43.3	42.8	44.0
Al_2O_3	11.9	12.6	12.5	12.1	12.0
FeO	6.9	6.7	6.9	6.7	6.3
MgO	17.0	16.5	16.6	16.1	16.4
TiO_2	2.2	1.8	1.7	2.5	3.4
CaO	11.5	12.0	11.9	12.1	11.5
Na_2O	2.4	2.4	2.4	2.4	2.5
K_2O	.9	1.0	.9	1.1	1.0
Cr_2O_3	.6	.7	.8	1.2	1.4
Cl	.29	n.d.	n.d.	n.d.	.13
F	.05	n.d.	n.d.	n.d.	.03
Total	97.64	97.22	97.0	97.0	98.5
Mineral formula calculated on the basis of 23 oxygens					
Si	6.315	6.310	6.294	6.241	6.285
Al^{IV}	1.685	1.690	1.706	1.759	1.715
Σ Tet	8.000	8.000	8.000	8.000	8.000
Al^{VI}	.359	.455	.431	.321	.303
Fe^{2+}	.838	.810	.837	.820	.755
Fe^{3+}	.000	.000	.000	.000	.000
Mg	3.677	3.554	3.593	3.500	3.494
Ti	.235	.201	.183	.273	.365
Cr	.072	.080	.095	.139	.161
Σ Oct	5.181	5.100	5.140	5.053	5.079
Excess Oct	.181	.100	.140	.053	.079
Ca	1.788	1.856	1.851	1.887	1.752
Na_B	.031	.043	.009	.059	.169
ΣB	2.000	2.000	2.000	2.000	2.000
Na_A	.648	.620	.654	.605	.515
K	.167	.178	.169	.208	.175
Σ A site	.814	.797	.823	.813	.690
$Mg/(Mg+Fe^{2+})$	.81	.81	.81	.81	.82
Accept[1]	Yes	Yes	Yes	Yes	Yes
Accept[2]	--	--	--	--	--
Name	Pargasitic hornblende	Pargasitic hornblende	Pargasitic hornblende	Pargasite	Pargasitic hornblende
Assemblage[3]	3	3	3	3	1

[1]Accepted, if:
1. Sum tetrahedral sites=8 ± 0.02
2. Sum octahedral sites >4.98
3. Excess octahedral site occupancy+Ca ≤2.02
4. Sum B site=2 ± 0.02
5. Sum A site ≤1.02
6. Residual charge <0.02

[2]Accepted, if:
1. Sum tetrahedral sites = 8 ± 0.02
2. Sum octahedral sites >4.97
3. Excess octahedral site occupancy+Ca ≤2.02
4. Sum B site=2 ± 0.02

[3]Assemblage
1. With chromite
2. With augite; no chromite
3. No spinel in rock
4. Others; combination; ambiguous

between the two groups being compared are statistically different for the confidence level being used (in this case 99.5 percent). The results of this test show that the hornblende compositions in rocks from the lower part of subunit 9 (group 3) are statistically higher in Fe, Na (in the A site), and total $(Na, K)_A$ and lower in Ti, Cr, and Na (in the M_4 site) than are the compositions of hornblende that rims chromite (group 1) or that replaces augite (group 2). Groups 1, 2, and 4 have nearly identical compositions.

On an expanded portion of the $Mg/(Mg + Fe^{2+})$ versus Si diagram of Leake (fig. 3*B*), the three groups of hornblende analyses form overlapping clusters of data. The hornblendes associated with chromite seem to be the most variable in composition. The composition of hornblende associated with augite decreases in $Mg/(Mg + Fe^{2+})$ as Si increases. The hornblendes from the lower portion of subunit 9 have a restricted range of composition and low $Mg/(Mg + Fe^{2+})$.

The compositional diversity of amphiboles can be most easily represented on cation-cation plots that emphasize some of the possible substitutions that take place within the amphibole structure. Two broad types of substitutions are possible: (1) exchange reactions, and (2) coupled substitutions. Exchange reactions include, for example, Fe and Mg exchange in the smaller M sites, Ca and Fe exchange in the M_4 site, or Na and K exchange in the A site. These exchanges do not require additional charge compensation. Coupled substitutions, however, require exchange of components in at least two structural sites in the amphibole to maintain charge balance. Examples of coupled substitutions

Table 3. Electron microprobe analyses and calculated mineral formulas of secondary amphiboles from the olivine cumulate of cyclic unit 2, Stillwater Complex, Montana
[Analyst: M.L. Zientek]

	618a-pt2	774a-pt1-core	774a-pt2-rim	774b-3,4	774c-pt5	774d-pt7	890b-pt1
Microprobe analyses, weight percent							
SiO_2	51.5	42.9	45.2	43.1	42.1	54.4	42.7
Al_2O_3	2.2	10.9	9.0	11.4	11.5	1.4	11.8
FeO	4.2	5.7	5.3	5.7	5.8	2.7	6.8
MgO	23.8	18.3	20.4	18.1	17.5	24.0	18.2
TiO_2	.00	1.5	.9	1.7	2.4	.2	1.7
CaO	11.3	11.4	10.9	11.5	11.2	12.4	11.4
Na_2O	.12	2.2	1.8	2.3	2.3	.44	2.4
K_2O	.00	.7	.19	.7	.9	.00	.8
Cr_2O_3	.00	1.6	1.0	1.7	1.6	.32	.78
Cl	.04	.31	.28	.30	.31	.00	.06
F	.00	.00	.01	.00	.03	.06	.01
Total	93.14	95.51	94.99	96.5	95.64	95.86	96.67
Mineral formula calculated on the basis of 23 oxygens							
Si	7.446	6.290	6.531	6.260	6.211	7.648	6.187
Al^{IV}	.368	1.710	1.469	1.740	1.789	.225	1.813
Σ Tet	7.814	8.000	8.000	8.000	8.000	7.873	8.000
Al^{VI}	.000	0.180	.060	.213	.201	.000	.199
Fe^{2+}	.170	.428	.097	.510	.686	.278	.487
Fe^{3+}	.334	.270	.545	.184	.030	.038	.331
Mg	5.120	3.990	4.392	3.916	3.854	5.025	3.939
Ti	.000	.160	.100	.183	.271	.016	.190
Cr	.000	.183	.112	.198	.191	.035	.089
ΣOct	5.252	5.211	5.306	5.204	5.232	5.139	5.232
Exess oct	.252	.211	.306	.204	.232	.139	.232
Ca	1.748	1.789	1.694	1.796	1.768	1.861	1.768
Na_B	.000	.000	.000	.000	.000	.000	.000
ΣB	2.000	2.000	2.000	2.000	2.000	2.000	2.000
Na_A	.034	.634	.516	.643	.652	.120	.663
K	.000	.123	.035	.137	.175	.000	.153
Σ A site	0.34	.757	.551	.780	.827	.120	.816
$Mg/(Mg+Fe^{2+})$	.97	.90	.98	.88	.85	.95	.89
Accept[1]	No	Yes	Yes	Yes	Yes	No	Yes
Accept[2]	--	--	--	--	--	No	--
Name	Tremolitic hornblende	Magnesio-hastingsitic hornblende	Edenitic hornblende	Pargasitic hornblende	Pargasite	Tremolite	Magnesio-hastingsite

[1]Accepted, if:
1. Sum tetrahedral sites=8 ± 0.02
2. Sum octahedral sites >4.98
3. Excess octahedral site occupancy+Ca ≤2.02
4. Sum B site=2 ±0.02
5. Sum A site ≤1.02
6. Residual charge <0.02

[2]Accepted, if:
1. Sum tetrahedral sites = 8 ±0.02
2. Sum octahedral sites >4.97
3. Excess octahedral site occupancy+Ca ≤2.02
4. Sum B site=2 ±0.02

[3]Assemblage
1. With chromite
2. With augite; no chromite
3. No spinel in rock
4. Others; combination; ambiguous

listed by the name previously assigned to them (Cameron and Papike, 1979) include the following:

1. $[\ ]_A + Si^{IV} = Na_A + Al^{IV}$ Edenite
2. $Mg^{VI} + Si^{IV} = Al^{VI} + Al^{IV}$ Tschermakite
3. $[\ ]_A + Ca_B = Na_A + Na_B$ Richterite
4. $Mg + Ca_B = Al^{VI} + Na_B$ Glaucophane

In the above equations, [ ] represents a vacancy in a site. Other substitutions are possible, such as tschermakite-type or glaucophane-type substitutions using Cr^{3+}, Fe^{3+}, or Ti^{4+} instead of Al^{VI} or Na_B.

The variations of hornblende compositions in cyclic unit 2 are displayed as cation-cation diagrams in figures 4, 5, and 6 and show the important coupled substitutions. The compositions of hornblendes in the assemblage groups are also compared on these plots and indicate that the hornblende

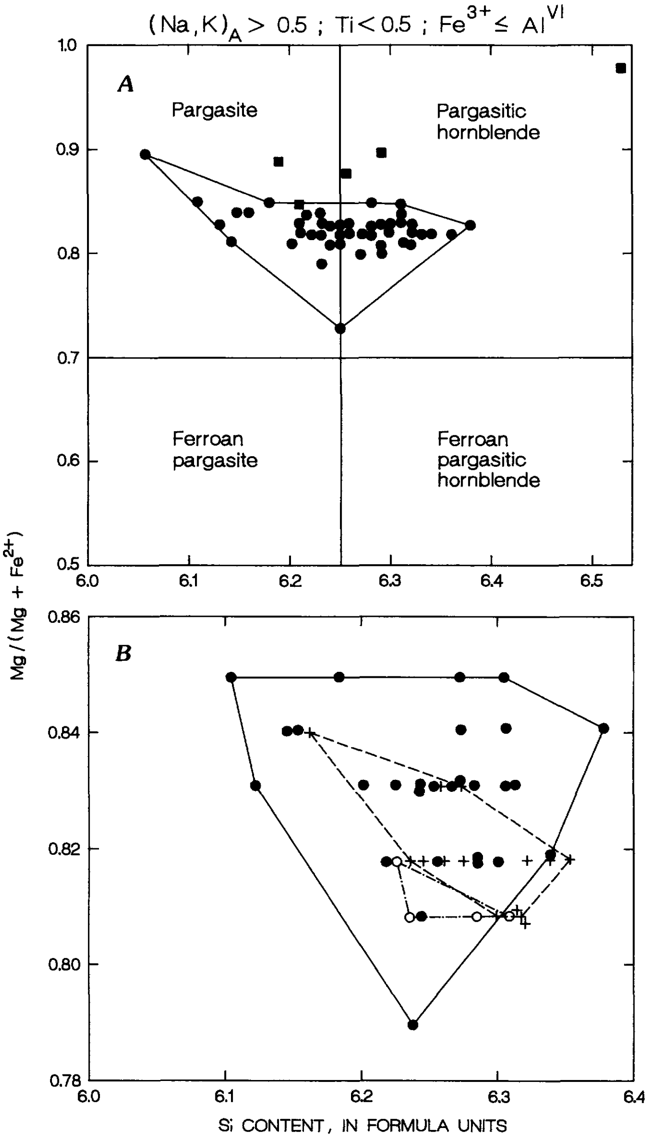

Figure 3. Classification and nomenclature of amphiboles. *A*, Calcic amphibole classification showing hornblende compositions (table 2; dots) and alteration amphiboles (table 3; squares). Some dots represent more than one analysis. *B*, Enlarged section of calcic amphibole classification diagram showing individual analyses for which textural assemblage could be determined (table 2). Hornblendes associated with chromite (dots) outlined in solid lines, with augite (circles) outlined by dash-dot line, and with no chromite (crosses) outlined by dashed lines.

compositions in the lower part of unit 9 (where spinel is not present) are distinct from those in augite- or chromite-related assemblages. On these plots, the assemblages of hornblende plus chromite are compared with the assemblages of hornblende plus augite and hornblende without any spinel in the rock (lower portion of subunit 9 in the cyclic unit).

Edenitic and tschermakitic coupled substitutions predominate (fig. 4). The end-member pargasite composition results from a linear combination of the tschermakite and edenite substitutions. It is obvious that charge imbalance created by the substitution of Na and K into the A site could be totally compensated by substitution of Al^{IV} into the tetrahedral sites. Al^{IV}, in excess of that required to offset Na and K substitution in the A site, almost compensates the charge imbalance created when trivalent and quadravalent cations substitute into the octahedral sites (fig. 5). This residual could be compensated by substitution of Na into the M_4 site (fig. 6). Glaucophane-like or riebiekite substitutions are most likely, although some richterite substitutions may be possible for those hornblendes in the lower portion of subunit 9, in which chromite is absent.

Hornblendes associated with chromite overlap the ranges of Al^{IV} and $(Na, K)_A$ (fig. 4) for the other textural assemblages, but they appear to have a broader range of Al^{IV} and $(Na, K)_A$ substitution than those hornblendes associated with augite or with no spinel (lower part of subunit 9). Hornblendes in the lower part of subunit 9 show distinct compositions when plotted on figures 4 and 5, an indication that there are lesser amounts of Al^{VI} + Ti + Cr in this group than in the other assemblages.

The variation in amounts of substitution in hornblende for Ti, Cr, and Al^{VI} in the different textural assemblages is illustrated on figure 7, where these cations are plotted versus Al^{IV}. The fields of hornblende compositions for the different textural assemblages overlap; however, hornblendes in rocks with no chromite from the lower portion of subunit 9 tend to have less Ti and Cr and more Al^{VI} than hornblendes in the other assemblages. Similarly, hornblendes from the lower portion of subunit 9 without chromite have lesser amounts of Na_B than hornblendes associated with augite or chromite (fig. 8).

In summary, the substitution mechanisms in hornblendes from cyclic unit 2 are dominated by tschermakitic- and edenitic-type substitutions that produce pargasite, with slightly more tschermakitic substitutions than edenitic substitutions. The substitution mechanisms are similar for hornblendes in each of the different textural assemblages, but hornblendes in the lower part of subunit 9 without chromite appear to be differentiated from the other assemblages by some richterite substitution and lesser amounts of Ti and Cr. The mean ratios of weight percent Cl to F in hornblendes associated with chromite and augite are 1.4 and 2.0, respectively, whereas the ratio in rocks from the lower portion of subunit 9 with no chromite is 6.0. Chlorine-to-fluorine ratios can be used to discriminate the hornblendes of the

Table 4. Means and standard deviations of hornblende analyses and formulas by assemblage groups

	Group 1			Group 2			Group 3			Group 4		
	Number of analyzed samples	Mean	Standard deviation	Number of analyzed samples	Mean	Standard deviation	Number of analyzed samples	Mean	Standard deviation	Number of analyzed samples	Mean	Standard deviation
						Microprobe analyses, weight percent oxides						
SiO_2------	32	42.9	0.57	15	42.9	0.48	5	43.3	0.47	23	42.9	0.47
Al_2O_3-----	32	12.1	.35	15	11.7	.40	5	12.3	.25	23	12.0	.37
FeO-------	32	5.9	.42	15	6.2	.25	5	6.9	.29	23	6.2	.37
MgO-------	32	16.0	.72	15	16.0	.55	5	16.6	.39	23	15.9	.46
TiO_2------	32	3.13	.47	15	2.99	.57	5	2.04	.31	23	2.89	.30
CaO-------	32	11.7	.33	15	11.6	.32	5	11.7	.38	23	11.7	.22
Na_2O------	32	2.4	.11	15	2.4	.10	5	2.4	.04	23	2.4	.14
K_2O-------	32	.96	.15	15	.90	.17	5	.94	.11	23	0.90	.15
Cr_2O_3----	32	1.4	.15	15	1.4	.24	5	.86	.23	23	1.4	.38
Cl--------	10	.10	.03	9	.14	.04	2	.18	.16	5	.15	.09
F---------	10	.07	.04	9	.07	.02	2	.03	.03	5	.06	.04
						Mineral formula calculated on the basis of 23 oxygens						
Si--------	32	6.252	0.069	15	6.287	0.050	5	6.277	0.041	23	6.276	0.051
Al^{IV}-----	32	1.748	.069	15	1.713	.050	5	1.723	.041	23	1.724	.051
Σ Tet-----	32	8.000	.000	15	8.000	.000	5	8.000	.000	23	8.000	.000
Al^{VI}------	32	.322	.082	15	.315	.085	5	.381	.059	23	.342	.053
Fe^{2+}------	32	.707	.070	15	.753	.031	5	.824	.013	23	.759	.045
Fe^{3+}------	32	.008	.043				5	.017	.038			
Mg--------	32	3.482	.135	15	3.483	.122	5	3.604	.083	23	3.464	.090
Ti--------	32	.342	.051	15	.330	.063	5	.223	.034	23	.318	.033
Cr--------	32	.166	.016	15	.165	.027	5	.098	.026	23	.156	.043
Σ Oct-----	32	5.026	.074	15	5.046	.069	5	.147	.079	23	5.039	.066
Excess Oct	32	.041	.061	15	.053	.063	5	.147	.079	23	.045	.059
Ca--------	32	1.829	.048	15	1.814	.046	5	1.824	.060	23	1.826	.035
Na B------	32	.130	.050	15	.132	.037	5	.028	.024	23	.129	.040
Σ B-------	32	2.00	.000	15	2.000	.00	5	2.00	.000	23	2.000	.000
Na A------	32	.550	.053	15	.550	.047	5	.636	.022	23	.562	.041
K---------	32	.179	.028	15	.167	.031	5	.175	.021	23	.169	.028
Σ A site--	32	.729	.046	15	.718	.043	5	.810	.010	23	.731	.030
X_{Mg}-------	32	.832	.017	15	.821	.009	5	.812	.004	23	.820	.010

lower part of subunit 9 in the olivine cumulates. A similar analysis of the compositions of the alteration amphiboles shows that the end product of the alteration process is a tremolitic hornblende or tremolite. Intermediate compositions are developed in single crystals in which the amphibole changes in composition from pargasite to tremolite. The major compositional changes are decreases in Al_2O_3, TiO_2, K_2O, Cr_2O_3, and perhaps Cl and F, and an increase in MgO. Alteration amphiboles are relatively rare in the samples studied.

COMPOSITION AND SUBSTITUTION MECHANISMS OF PHLOGOPITE

Phlogopite is used to refer to a trioctahedral mica in which most of the octahedral positions are occupied by Mg (Foster, 1960). For the analyses in table 6, 70 to 80 percent of the octahedral positions are occupied by Mg. Normally, phlogopites have less than 0.10 cation positions occupied by Ti (Foster, 1960); however, the calculated formulas for phlogopites from the olivine cumulates generally contain more than 0.2 formula units Ti, with a range from 0.095 to 0.347. With two exceptions, all analyses in table 6 contain greater than 3.0 weight percent TiO_2; in addition, they all have Al^{VI} that is less than Al^{IV} (with the Al^{VI} also accompanied by a Si deficiency) and a K-site deficiency of less than 0.2. Because it was not possible to determine Fe_2O_3, the analyses when cast as end members plot as combinations of phlogopite, annite, and siderophyllite (fig. 9). The phlogopite compositions form a relatively tight cluster between 72 and 80 percent phlogopite end member, with about equal proportions of annite and siderophyllite.

Various substitution mechanisms have been suggested for phlogopites, including the phlogopite-annite series (K_2Mg_6 [$Si_6Al_2O_{20}$] $(OH)_4$ to K_2Fe_6 [$Si_6Al_2O_{20}$] $(OH)_4$) and the phlogopite-siderophyllite series (K_2Mg_6 [$Si_6Al_2O_{20}$] $(OH)_4$ to $K_2Fe_5Al^{VI}$ [$Si_5Al_3^{IV}O_{20}$] $(OH)_4$); both of these substitution mechanisms seem to operate in the phlogopites of the olivine cumulates (see fig. 9). Arima and Edgar (1981), among others, have examined the possible substitution mechanisms involving Ti in phlogopite, and the discussion that follows is based on their calculation and plotting methodology.

In figure 10, all the phlogopite analyses have Al^{VI} less than Al^{IV} and enough Al to compensate for the Si deficiency so that no Fe^{+3} or Ti^{IV} is needed. They cluster on a line between two end members, $K_2Mg_5TiAl_4Si_4O_{20}(OH)_4$ and K_2Mg_4 [ ] $TiAl_2Si_6O_{20}(OH)_2$, indicating that Ti is likely to occupy the octahedral site. The phlogopites have trends of increasing Ti with both octahedral site occupancy and Si + Al^{VI}, as shown in figure 11. This relation suggests that the two substitution mechanisms, $2Mg^{VI} \rightleftharpoons Ti^{VI}$ and $Mg^{VI}2Si^{IV} \rightleftharpoons Ti^{VI}2Al^{IV}$, are operative in the Stillwater phlogopites.

Table 5. Comparison of the differences in means between assemblage groups given in table 4
[Comparison criteria are calculated for 99.5-percent confidence level]

	Group 1						Group 2				Group 3	
	Group 2		Group 3		Group 4		Group 3		Group 4		Group 4	
	Mean difference	Comparison criteria	Mean difference	Comparison criteria	Mean difference	Comparison criteria	Mean difference	Comparison criteria	Mean difference	Comparison criteria	Mean difference	Comparison criteria
Microprobe analyses, weight percent												
SiO_2-------	0.016	0.456	0.345	0.732	0.028	0.385	0.329	0.707	0.044	1.893	0.373	0.649
Al_2O_3------	.307	.298	.222	.425	.075	.253	.529	.549	.232	1.659	.297	.485
FeO--------	.281	.318	1.051	.537	.334	.292	.770	.386	.053	1.801	.717	.493
MgO--------	.080	.568	.594	.912	.157	.456	.675	.767	.077	1.855	.751	.622
TiO_2-------	.134	.424	1.089	.598	.236	.295	.956	.775	.103	1.549	.853	.410
CaO--------	.150	.272	.005	.437	.069	.209	.145	.488	.081	1.281	.064	.345
Na_2O-------	.002	.092	.052	.139	.028	.090	.050	.136	.030	1.080	.080	.177
K_2O--------	.068	.129	.022	.188	.059	.107	.046	.231	.009	1.043	.037	.196
Cr_2O_3------	.005	.154	.570	.214	.074	.197	.575	.346	.079	1.871	.496	.495
Cl---------	.045	.051	.081	.140	.051	.093	.036	.148	.006	0.924	.030	.329
F----------	.000	.042	.036	.093	.002	.063	.036	.042	.002	.575	.034	.105
Mineral formula calculated on the basis of 23 oxygens												
Si---------	0.035	0.053	0.025	0.087	0.024	0.045	0.010	0.071	0.011	0.618	0.001	0.068
Al^{IV}-------	.035	.053	.025	.087	.024	.045	.010	.071	.011	.618	.001	.068
ΣTet-------	.000	.000	.000	.000	.000	.000	.000	.000	.000	.000	.000	.000
Al^{VI}-------	.006	.070	.059	.105	.020	.052	.065	.119	.027	.630	.039	.074
Fe^{2+}-------	.046	.051	.117	.087	.052	.044	.071	.042	.006	.618	.065	.057
Fe^{3+}-------	.008	--	.009	--	.008	--	.017	--	.000	--	.017	--
Mg---------	.002	.110	.123	.170	.018	.086	.121	.168	.020	.810	.141	.122
Ti---------	.013	.047	.119	.065	.024	.032	.107	.086	.012	.511	.095	.045
Cr---------	.000	.017	.067	.023	.009	.022	.067	.040	.009	.625	.058	.056
Σ Oct------	.020	.061	.121	.098	.013	.051	.101	.106	.008	.694	.108	.093
Excess Oct-	.011	.052	.106	.083	.004	.044	.094	.099	.008	.656	.102	.085
Ca---------	.014	.040	.004	.065	.002	.031	.010	.072	.012	.506	.002	.055
Na_B--------	.002	.039	.102	.063	.001	.034	.104	.051	.004	.548	.100	.052
Σ B--------	.000	.000	.000	.000	.000	.000	.000	.000	.000	.000	--	--
Na_A--------	.001	.043	.086	.067	.012	.035	.085	.063	.012	.545	.074	.053
K----------	.012	.024	.004	.036	.010	.020	.007	.043	.001	.451	.006	.037
Σ A site---	.011	.038	.081	.057	.002	.029	.092	.056	.013	.466	.079	.038
X_{Mg}--------	.011	.013	.020	.022	.011	.011	.009	.012	.000	.272	.008	.013

Comparison criteria = t (s $(1/n_1 + 1/n_2)$) where:
t is the value of a test statistic derived from Students' t-distribution for a level of significance of 99.5 percent,
n_1 and n_2 are the sample sizes of the two populations,
s is the pooled standard deviation and is equal to

$$\sqrt{\frac{(n_1-1)\,s_1^2 + (n_2-1)\,s_2^2}{n_1 + n_2^{-2}}}$$

, where s_1 and s_2 are the standard deviations of the two populations.

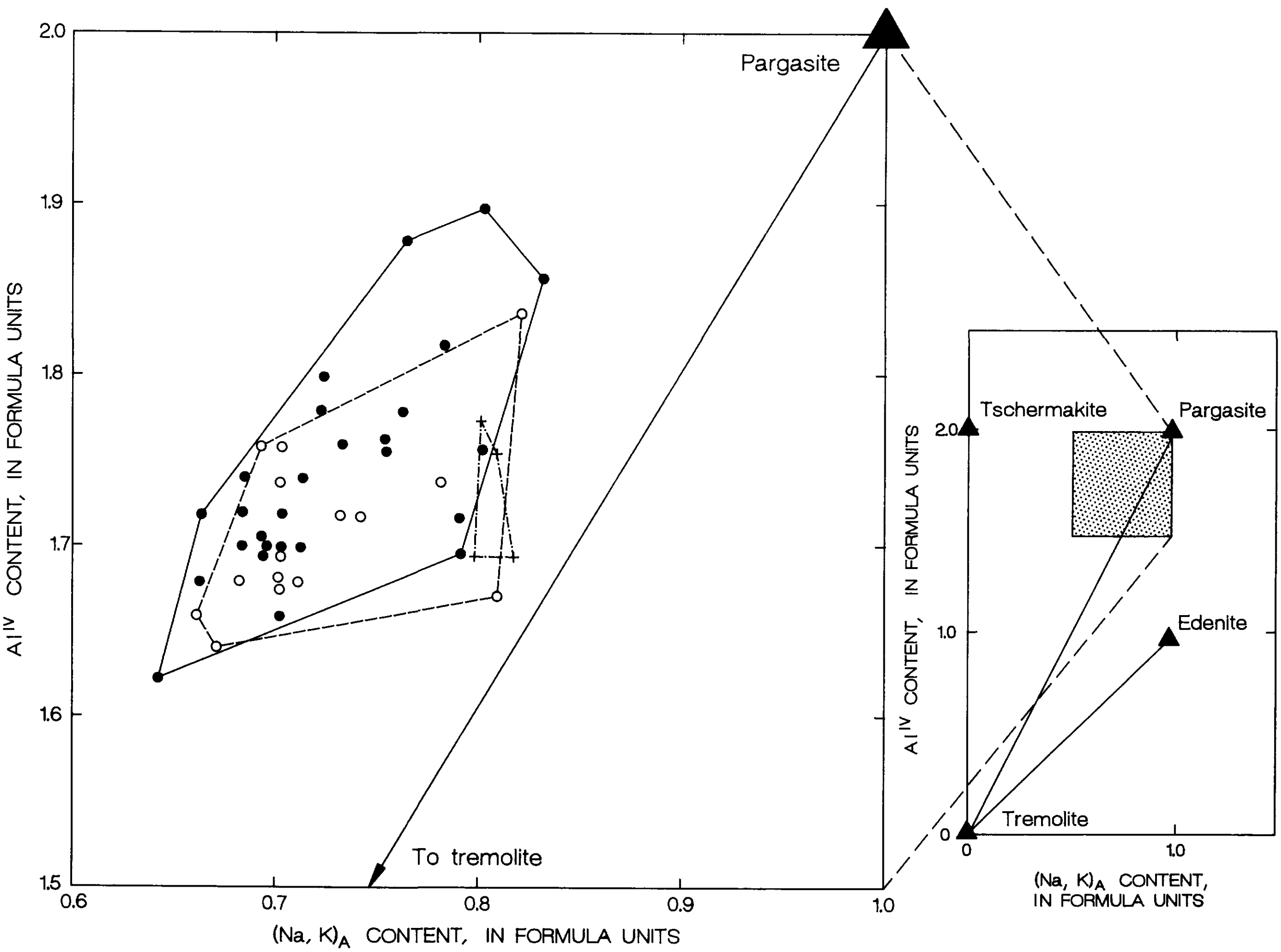

Figure 4. Plot of Al^{IV} versus (Na, K)$_A$ for hornblendes in table 2, divided into textural assemblages and an end-member diagram. Symbols are same as in figure 3.

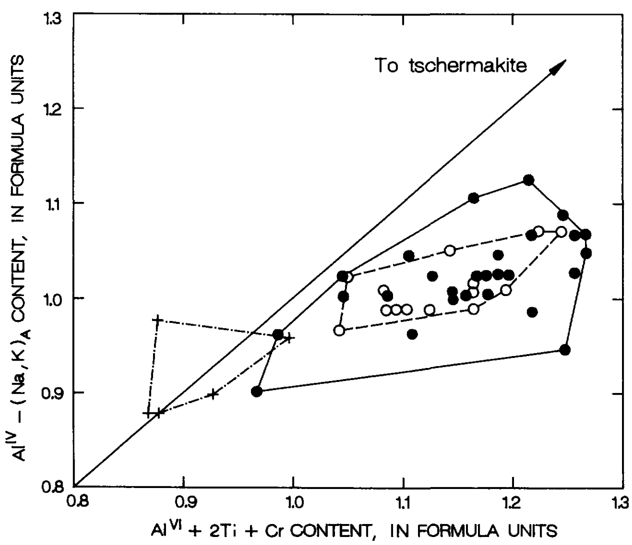

Figure 5. Al^{IV} – (Na, K)$_A$ versus Al^{VI} + 2Ti + Cr for hornblendes in table 2, divided into textural assemblages. Symbols are same as in figure 3.

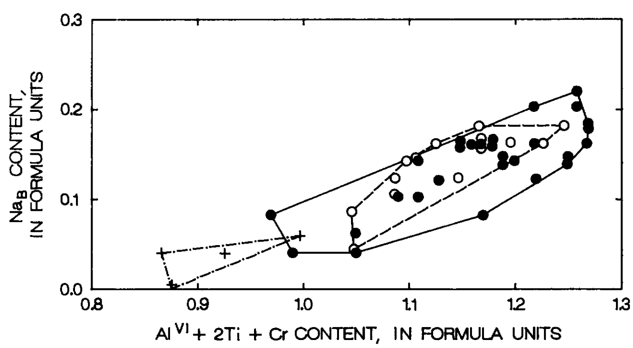

Figure 6. Na_B versus Al^{VI} + 2Ti + Cr for hornblendes in table 2, divided into textural assemblages. Symbols are same as in figure 3.

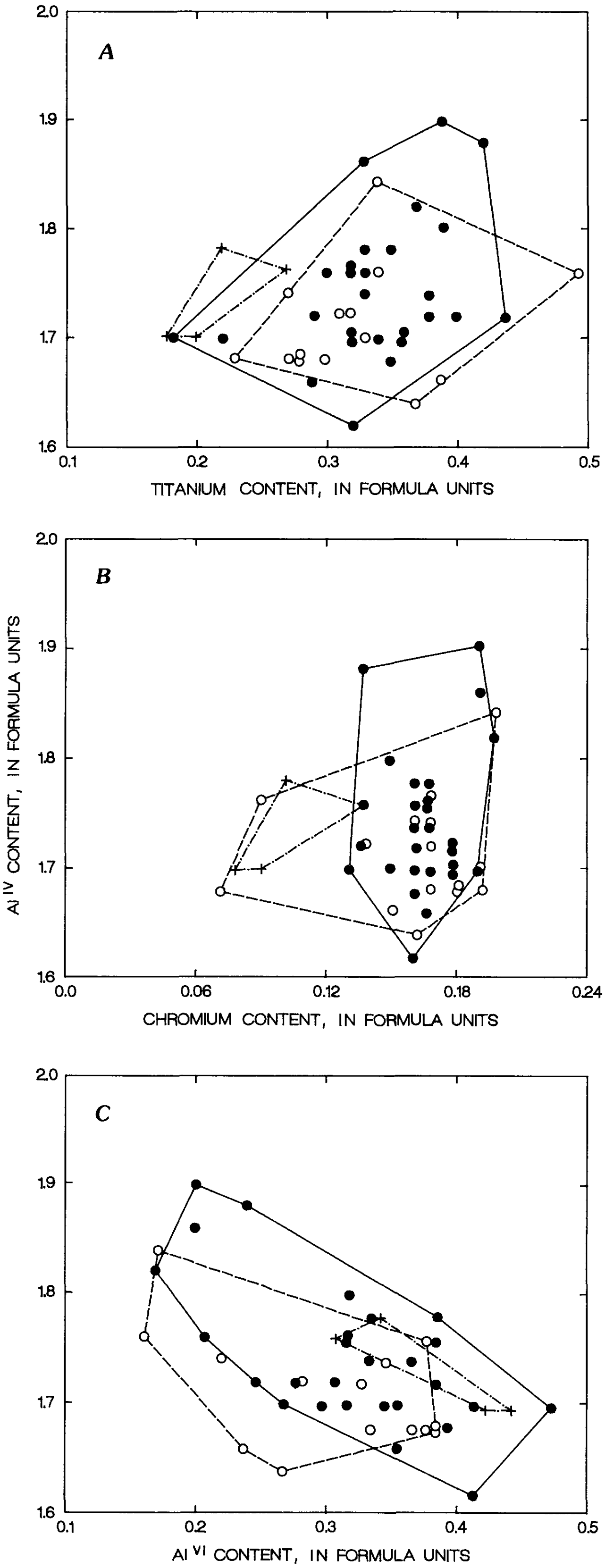

Figure 7. Al^{IV} versus Ti, Cr, and Al^{VI} for hornblendes in table 2, divided into textural assemblages. Symbols are same as in figure 3. *A*, Al^{IV} versus Ti. *B*, Al^{IV} versus Cr. *C*, Al^{IV} versus Al^{VI}.

ASSEMBLAGE-CONTROLLED COMPOSITIONAL VARIATIONS IN BROWN AMPHIBOLE

Two facets of the composition information warrant further discussion. First, is there any compositional difference between the various distinct textural assemblages of brown amphibole within single samples? Second, is there any systematic variation in the composition of single hornblende crystals related to the coexisting assemblage?

Compositional Variation Between Assemblage Groups Within the Same Sample

Although the analysis presented in the previous section indicates there was little difference in composition between hornblendes in different assemblages taken as a whole, the compositional range may have obscured any systematic variation that might have existed within individual samples, here defined as a single thin section. The recognition of hornblende assemblages with different compositions within individual samples is important in any interpretation of hornblende compositions as a function of stratigraphic position.

Comparison of hornblende analyses for different textural assemblages in a single sample show that there is a systematic difference based on assemblage when examined on cation-cation plots. Hornblende associated with chromite

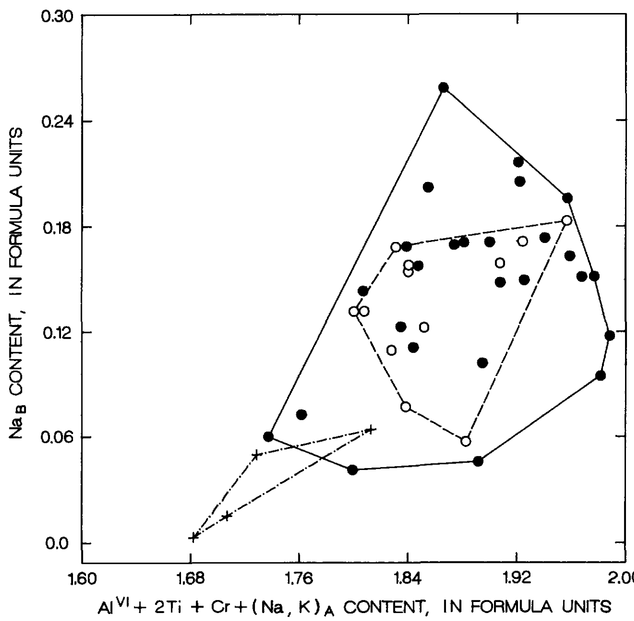

Figure 8. Na_B versus Al^{VI} + 2Ti + Cr + $(Na, K)_A$ for hornblendes in table 2, divided into textural assemblages. Symbols are same as in figure 3.

Table 6. Electron microprobe analyses and calculated mineral formulas of phlogopite from the olivine cumulate of cyclic unit 2, Stillwater Complex, Montana

[Analyst: M.L. Zientek, n.d., not determined; ph, phlogopite; an, annite; sid, siderophyllite]

	623c	628a	630c	630a	685a-bt1	685a-bt2	690d	691.5c-btl	691.5c-bt2	701a-bt1	701a-bt2	715a
Microprobe analyses, weight percent												
SiO_2	38.7	36.9	37.6	37.8	38.2	38.0	38.0	38.5	38.4	37.2	38.2	38.1
Al_2O_3	15.4	13.2	15.4	15.5	15.8	15.9	16.1	16.2	16.3	15.5	15.7	15.7
TiO_2	5.0	4.6	5.2	5.6	3.5	3.6	3.3	1.8	3.6	4.7	4.7	4.7
FeO	5.6	4.7	6.0	6.2	6.0	5.9	5.8	5.5	5.9	6.0	6.0	6.0
MgO	20.1	20.5	19.6	19.3	20.3	20.2	21.1	21.7	20.3	19.3	19.2	19.5
Cr_2O_3	1.1	1.0	1.2	1.2	1.4	1.5	1.0	.8	1.1	1.4	1.4	1.2
CaO	.00	.30	.00	.31	.00	.00	.00	.00	.01	.02	.00	.00
Na_2O	.5	.5	.8	.8	.9	.9	.5	1.3	1.1	1.1	1.1	.6
K_2O	9.3	9.9	9.6	9.1	9.3	9.1	9.6	8.7	8.9	8.8	8.8	9.5
F	.01	.00	.01	.00	.07	.08	n.d.	.02	.05	.08	.11	.02
Cl	.07	.04	.18	.17	.31	.33	n.d.	.41	.34	.26	.26	.35
Total	95.78	91.64	95.59	95.97	95.78	95.51	95.4	94.93	96.00	94.36	95.47	95.67
Formula based on sum of positive charges=22												
Si	2.766	2.774	2.717	2.718	2.756	2.747	2.736	2.777	2.747	2.729	2.758	2.749
Al^{IV}	1.234	1.226	1.283	1.282	1.244	1.253	1.264	1.223	1.253	1.271	1.242	1.251
Al^{VI}	.065	.000	.033	.033	.095	.102	.104	.155	.126	.065	.094	.081
Ti	.269	.261	.285	.304	.192	.195	.177	.095	.193	.256	.253	.257
Fe^{2+}	.336	.293	.362	.371	.362	.359	.347	.334	.352	.367	.363	.362
Mg	2.139	2.300	2.114	2.063	2.182	2.182	2.260	2.332	2.171	2.105	2.072	2.098
Cr	.032	.030	.034	.035	.041	.042	.029	.022	.032	.041	.039	.035
ΣOct	2.841	2.884	2.829	2.806	2.872	2.879	2.917	2.937	2.873	2.835	2.820	2.834
Ca	.00	.024	.00	.024	.00	.00	.00	.00	.001	.002	.00	.00
Na	.069	.073	.105	.113	.123	.121	.066	.182	.146	.156	.154	.081
K	.845	.948	.881	.833	.857	.843	.878	.800	.817	.824	.809	.872
F	.002	.00	.002	.00	.016	.018	n.d.	.005	.011	.019	.025	.005
Cl	.009	.005	.022	.021	.038	.040	n.d.	.050	.041	.032	.032	.043
OH	1.989	1.995	1.976	1.979	1.946	1.941	n.d.	1.945	1.947	1.949	1.943	1.953
Xmg	.75	.81	.75	.74	.76	.76	.77	.79	.76	.74	.73	.74
F/F+OH	.001	.00	.001	.00	.008	.009	n.d.	.002	.006	.009	.013	.002
Cl/Cl+OH	.004	.003	.011	.010	.019	.020	n.d.	.025	.021	.016	.016	.021
log (F/OH)	-2.998	.00	-2.936	.00	-2.086	-2.026	n.d.	-2.630	-2.236	-2.022	-1.888	-2.632
log (Cl/OH)	-2.344	-2.592	-1.952	-1.981	-1.711	-1.681	n.d.	-1.589	-1.674	-1.781	-1.786	-1.659
Xph	.75	.81	.75	.74	.76	.76	.77	.79	.76	.74	.73	.74
Xan	.12	.12	.12	.12	.11	.11	.10	.90	.10	.12	.12	.12
Xsid	.12	.07	.14	.14	.13	.13	.13	.12	.14	.14	.14	.14

	730b	747a	755b	755b b	755bc	755ca	767b	787b-bt1	787b-bt2	815a	830ab	861b	874a
Microprobe analyses, weight percent													
SiO_2	38.0	37.8	38.5	38.0	38.6	37.3	38.1	39.0	38.5	37.7	37.8	38.0	37.6
Al_2O_3	15.8	15.3	15.6	15.3	15.3	15.4	15.7	16.2	15.9	16.1	15.8	15.7	15.4
TiO_2	4.4	5.1	3.4	3.7	4.5	6.4	3.5	4.2	5.2	2.9	5.2	5.2	5.4
FeO	5.2	5.3	5.5	6.4	5.9	5.6	4.7	4.8	4.5	5.2	5.2	5.2	4.0
MgO	20.9	20.6	20.7	20.4	20.7	19.7	21.8	20.4	20.5	21.0	19.7	20.0	21.3
Cr_2O_3	1.0	1.0	.7	1.0	.8	1.1	1.0	1.2	1.3	1.5	1.3	1.2	1.1
CaO	.00	.00	.00	.00	.00	.00	.00	.00	.02	.00	.03	.00	.00
Na_2O	.5	.5	1.0	.7	.9	.7	.7	.8	.7	.6	.7	.5	.7
K_2O	9.4	9.4	9.0	8.8	8.9	9.0	9.0	9.4	9.5	9.5	9.6	9.5	9.3
F	n.d.	n.d.	.11	n.d.	n.d.	n.d.	n.d.	.02	.02	n.d.	.01	n.d.	n.d.
Cl	n.d.	n.d.	.28	n.d.	n.d.	n.d.	n.d.	.05	.06	n.d.	.07	n.d.	n.d.
Total	95.2	95.0	94.79	94.3	95.6	95.2	94.5	96.07	96.20	94.5	95.41	95.3	94.7
Formula based on sum positive charges=22													
Si	2.730	2.724	2.781	2.761	2.758	2.690	2.744	2.773	2.738	2.744	2.724	2.730	2.705
Al^{IV}	1.270	1.295	1.270	1.276	1.219	1.239	1.242	1.310	1.256	1.227	1.262	1.256	1.276
Al^{VI}	.071	.023	.111	.073	.049	.000	.079	.130	.070	.121	.064	.063	.013
Ti	.236	.277	.187	.204	.243	.347	.187	.223	.276	.157	.283	.281	.294
Fe^{2+}	.315	.322	.334	.389	.352	.337	.284	.286	.268	.317	.315	.310	.240
Mg	2.236	2.216	2.222	2.209	2.208	2.116	2.345	2.154	2.174	2.277	2.115	2.148	2.283
Cr	.028	.029	.020	.029	.021	.032	.029	.035	.036	.042	.037	.034	.030
ΣOct	2.886	2.867	2.873	2.904	2.874	2.832	2.923	2.829	2.823	2.912	2.815	2.834	2.860
Ca	.00	.00	.00	.00	.00	.00	.00	.00	.002	.00	.002	.00	.00
Na	.063	.074	.141	.102	.125	.094	.096	.109	.094	.078	.094	.070	.092
K	.863	.861	.827	.819	.813	.832	.831	.848	.862	.879	.879	.873	.851
F	n.d.	n.d.	.025	n.d.	n.d.	n.d.	n.d.	.004	.005	n.d.	.002	n.d.	n.d.
Cl	n.d.	n.d.	.034	n.d.	n.d.	n.d.	n.d.	.006	.007	n.d.	.009	n.d.	n.d.
OH	n.d.	n.d.	1.941	n.d.	n.d.	n.d.	n.d.	1.989	1.988	n.d.	1.989	n.d.	n.d.
Xmg	.77	.77	.77	.76	.77	.75	.80	.76	.77	.78	.75	.76	.80
F/F+OH	n.d.	n.d.	.013	n.d.	n.d.	n.d.	n.d.	.002	.002	n.d.	.001	n.d.	n.d.
Cl/Cl+OH	n.d.	n.d.	.017	n.d.	n.d.	n.d.	n.d.	.003	.004	n.d.	.004	n.d.	n.d.
log (F/OH)	n.d.	n.d.	-1.888	n.d.	n.d.	n.d.	n.d.	-2.646	-2.645	n.d.	-2.940	n.d.	n.d.
log (Cl/OH)	n.d.	n.d.	-1.753	n.d.	n.d.	n.d.	n.d.	-2.519	-2.439	n.d.	-2.366	n.d.	n.d.
Xph	.77	.7	.77	.76	.77	.75	.80	.76	.77	.78	.75	.76	.80
Xan	.10	.11	.11	.12	.12	.12	.09	.11	.11	.90	.11	.11	.09
Xsid	.12	.12	.12	.12	.11	.14	.11	.13	.12	.13	.14	.13	.11

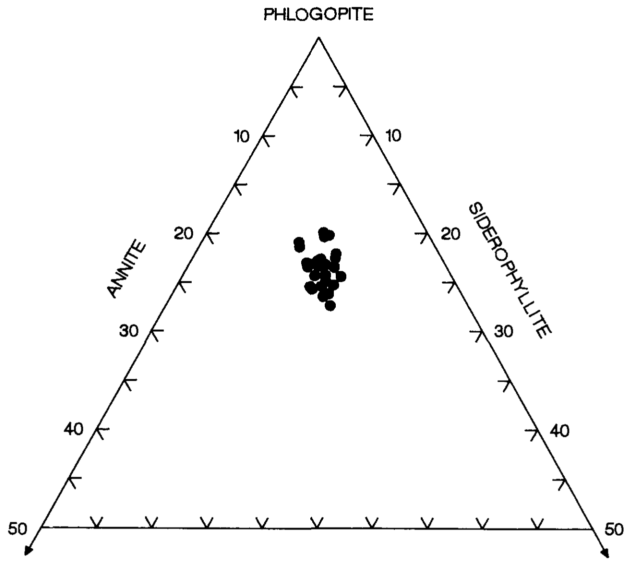

Figure 9. Phlogopite compositions, in percent, from olivine cumulate of cyclic unit 2 cast as phlogopite, annite, and siderophyllite end members.

shows a larger extent of coupled substitution and may be slightly more magnesium rich. The compositional variation between different assemblages within single samples is similar to the variations found in the whole group of samples, and the same substitution mechanisms predominate.

Compositional Variation Among the Assemblage Groups Within the Same Hornblende Crystal

In order to understand variations in hornblende compositions in the chromite-associated assemblage and the extent of coupled substitutions involving individual elements, three samples were selected to study composition zoning in single crystals. In each sample, the hornblende crystal was large enough so that it was in contact with a variety of silicate and (or) oxide crystals. The compositions of the hornblende in contact with each adjoining phase were then determined,

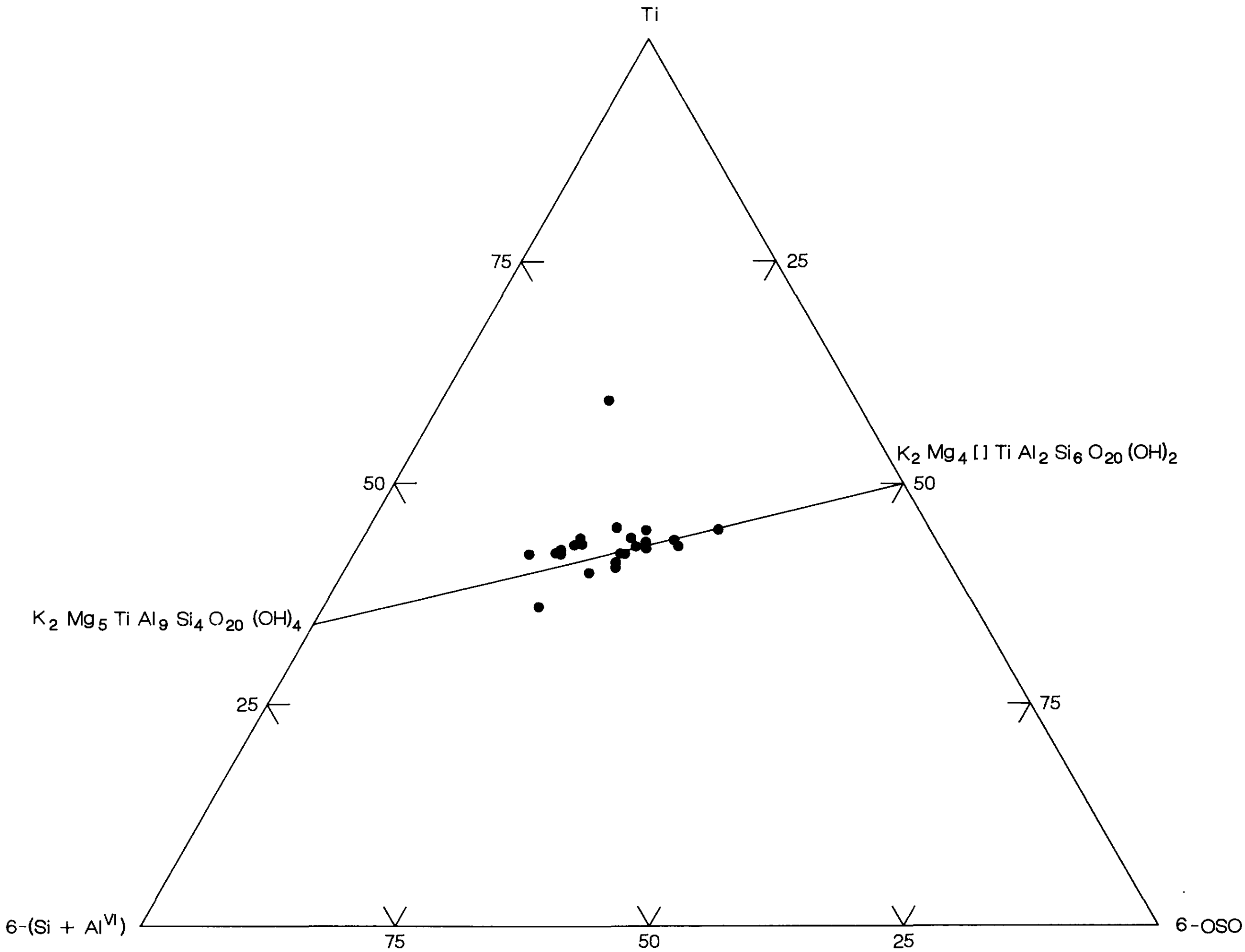

Figure 10. Phlogopite compositions, in percent, in terms of Ti, 6-OSO (octahedral site occupancy), and 6-(Si + Al^{VI}) in structural formula.

and the results are presented in table 7. In addition, the compositions of the coexisting chromite and olivine were analyzed; these analyses are given in tables 8 and 9, respectively. Sketches of the areas examined, with the locations of the points analyzed, are shown in figure 12. The results show that the crystals are zoned and that the composition of the hornblende is related to the composition of the chromite.

Although the samples come from different stratigraphic positions in the olivine cumulate of cyclic unit 2, Mg/(Mg + Fe^{2+}) of the olivine crystals is the same (0.85). This ratio reflects the composition of olivine in the core of crystals; no large-scale zoning was recognized. The spinels are chromites with Mg/(Mg + Fe^{2+}) between 0.329 and 0.412 and with Cr/(Cr + Al) between 0.546 and 0.596. TiO_2 varies from 0.76 to 2.2 weight percent. In one sample (747b), the rims tend to be slightly Mg enriched.

Two approaches to examining the hornblende data in table 7 were used. One was to look at cation contents plotted spatially with respect to the adjacent chromite and silicate minerals, and the other was to examine cation-cation plots to evaluate the amounts and types of substitution.

The distribution of cation and selected cation ratios is shown for the three samples containing zoned hornblendes (fig. 12). Mg/(Mg + Fe^{2+}) in hornblende does not vary by more than 0.03 units in any of the three samples nor does its variation appear to be related systematically to the adjoining chromites and silicates. However, variations in the cation proportions of Cr and Ti (fig. 12*B*, *C*) are more strongly influenced by the adjoining minerals to the amphibole. The best example of this relation is the distribution of Ti in sample 747b (fig. 12*C*). In this sample, the Ti content (formula units) of amphibole next to olivine and plagioclase is 0.29 to 0.32, whereas the Ti contents of amphibole next to chromite and plagioclase and of amphibole next to chromite and olivine range from 0.36 to 0.38 and 0.35 to 0.38, respectively. Similar, although not as strong, correlations are found in samples 830a and 755c. Cation units of Cr are the highest next to chromite plus plagioclase or chromite plus olivine and are the lowest next to plagioclase plus olivine (fig. 12*B*). These observations strongly suggest that Cr and Ti zoning in hornblende is influenced by the nearest neighbor minerals to the hornblende. The distribution of Al^{IV} cations (fig. 12*D*) in hornblende also appears to be influenced by the adjoining minerals. Hornblende in contact with chromite and plagioclase has higher amounts of Al^{IV} than hornblende in contact with other combinations of minerals. The distribution of Al^{VI} in hornblendes appears to be lower in hornblende in contact with chromite (fig. 12*E*). Examination of the distribution of $(Na, K)_A$ and Na_B cations in the hornblendes suggests that their distribution is not influenced by the adjoining minerals, except that there is a suggestion that Na_B cations are lowest in hornblende that is in contact with plagioclase and olivine. In summary, both chromite and silicate minerals appear to be related to changes in composition of the zoned brown amphiboles, and the presence or absence of chromite seems to affect the composition more than the presence or absence of silicates.

Changes in the composition of the zoned hornblendes depending on assemblage were also examined on cation-cation plots similar to those in figures 3–8. Based on this examination, it was concluded that the substitution mechanisms for these zoned crystals are the same as those discussed earlier for all hornblendes. As might be expected, hornblende adjacent to chromite-bearing assemblages has a greater extent of coupled substitution of edenite and tschermakite and higher Ti and Na_B contents. Cr content is

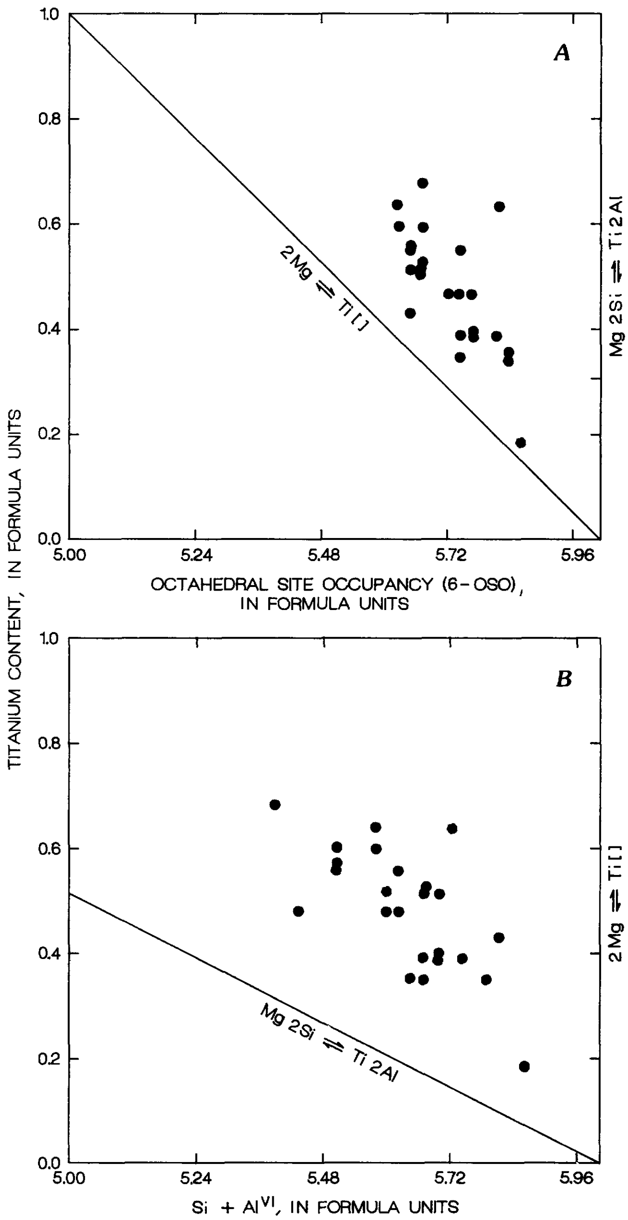

Figure 11. Phlogopite compositions. *A*, Ti versus 6-OSO. *B*, Ti versus Si + Al^{VI}.

Table 7. Electron microprobe analyses and calculated mineral formulas of zoned amphibole crystals from the olivine cumulate of cyclic unit 2, Stillwater Complex, Montana
[Analyst: M.L. Zientek]

	747b-pt1	747b-pt7	747b-pt8	747b-pt2	747b-pt9	747b-pt3	747b-pt10	747b-pt11	747b-pt12	747b-pt4	747b-pt13	747b-pt14
Microprobe analyses, weight percent												
SiO_2------	43.2	42.9	43.7	42.3	43.3	42.7	42.1	42.0	42.3	43.3	43.7	43.5
Al_2O_3-----	12.3	12.2	11.9	12.2	12.2	12.4	12.5	12.7	12.4	11.6	11.2	11.8
FeO-------	5.9	6.3	6.1	5.8	5.8	5.7	5.7	6.2	5.6	5.8	5.4	6.0
MgO-------	16.5	17.1	16.6	16.2	16.3	16.4	16.4	16.2	16.5	16.6	16.9	16.4
MnO-------	.08	.11	.09	.07	.08	.08	.05	.35	.07	.08	.05	.07
TiO_2------	2.7	2.7	3.0	3.4	3.5	3.5	3.5	3.3	3.5	3.5	3.5	3.3
CaO-------	12.3	11.9	12.1	12.1	12.2	12.2	12.2	11.7	12.1	12.0	12.2	12.2
Na_2O------	2.3	2.3	2.7	2.6	2.6	2.6	2.6	2.6	2.6	2.7	2.6	2.0
K_2O-------	.89	.87	.83	.96	.88	.95	.91	.96	.91	.82	.85	.85
Cr_2O_3-----	.98	.94	1.2	1.5	1.6	1.6	1.6	1.6	1.6	1.5	1.5	1.4
Total--	97.10	97.32	98.22	97.13	98.45	98.13	97.56	97.61	97.58	97.90	97.90	97.52
Mineral formula calculated on the basis of 23 oxygens												
Si-------	6.252	6.215	6.263	6.149	6.205	6.140	6.095	6.086	6.113	6.225	6.272	6.272
Al^{IV}-----	1.748	1.785	1.737	1.851	1.795	1.860	1.905	1.914	1.887	1.775	1.728	1.728
ΣTet-----	8.000	8.000	8.000	8.000	8.000	8.000	8.000	8.000	8.000	8.000	8.000	8.000
Al^{VI}-----	.349	.299	.282	.241	.265	.241	.228	.265	.299	.196	.167	.278
Fe^{2+}-----	.711	.767	.731	.700	.694	.682	.687	.757	.675	.701	.651	.726
Mg-------	3.555	3.684	3.544	3.508	3.475	3.518	3.532	3.507	3.556	3.565	3.619	3.523
Mn-------	.010	.013	.011	.009	.010	.010	.006	.043	.009	.010	.006	.008
Ti-------	.294	.289	.325	.372	.376	.382	.385	.361	.380	.382	.373	.354
Cr-------	.112	.108	.133	.177	.175	.179	.180	.178	.185	.172	.175	.163
ΣOct-----	5.031	5.160	5.025	5.007	4.996	5.011	5.018	5.111	5.034	5.025	4.991	5.053
Excess Oct	.031	.160	.025	.007	.00	.011	.018	.111	.034	.025	.000	.053
Ca-------	1.909	1.840	1.866	1.878	1.866	1.875	1.898	1.813	1.880	1.848	1.883	1.875
Na_B------	.060	.000	.109	.115	.134	.113	.084	.076	.086	.126	.117	.072
ΣB-------	2.000	2.000	2.000	2.000	2.000	2.000	2.000	2.000	2.000	2.000	2.000	2.000
Na_A------	.594	.640	.631	.626	.583	.615	.643	.647	.631	.620	.618	.495
K--------	.164	.161	.152	.178	.161	.174	.168	.178	.168	.150	.156	.156
ΣA site--	.759	.801	.783	.803	.743	.790	.811	.825	.799	.770	.774	.651
$Mg/(Mg+Fe^{2+})$	.83	.83	.83	.83	.83	.84	.84	.82	.84	.84	.85	.83
Accept[1]	yes	yes	yes	yes	yes	yes	yes	yes	yes	yes	yes	yes
Name-----	Pargasitic hornblende	Pargasite	Pargasitic hornblende	Pargasite	Pargasite	Pargasite	Pargasite	Pargasite	Pargasite	Pargasite	Pargasitic hornblende	Pargasitic hornblende

Table 7. Electron microprobe analyses and calculated mineral formulas of zoned amphibole crystals from the olivine cumulate of cyclic unit 2, Stillwater Complex, Montana—*Continued*

	755ca-pt1	747ca-pt5	755ca-pt6	755ca-pt7	755ca-pt8	755ca-pt4	755ca-pt9	755ca-pt10	755ca-pt2	755ca-pt11	755ca-pt12	755ca-pt13
	Microprobe analyses, weight percent											
SiO_2-----	43.0	43.1	42.7	42.6	42.2	43.0	43.3	43.2	543.4	42.8	43.6	43.1
Al_2O_3----	11.9	11.7	12.1	11.6	12.5	11.6	11.5	11.6	11.9	12.0	12.0	12.0
FeO------	6.1	6.6	6.1	5.8	6.3	6.0	5.8	5.9	6.0	6.5	6.0	6.0
Mgo------	16.3	16.4	16.3	16.4	15.9	16.0	16.3	16.4	16.4	16.6	16.5	16.2
MnO------	.08	.10	.08	.07	.10	.07	.08	.08	.06	.08	.06	.07
TiO_2-----	3.3	3.3	3.3	4.2	4.2	4.3	4.3	4.4	3.1	3.1	3.0	3.2
CaO------	11.8	11.8	12.0	12.0	11.9	11.8	12.0	11.9	11.8	11.7	12.0	11.8
Na_2O-----	2.8	2.9	2.7	2.9	2.7	2.8	2.4	2.9	2.6	2.7	2.7	2.8
K_2O------	.69	.66	.54	.62	.84	.62	.52	.61	.77	.66	.73	.71
Cr_2O_3----	1.4	1.5	1.4	1.4	1.3	1.4	1.4	1.4	1.4	1.4	1.5	1.6
Total--	97.37	98.06	97.22	97.59	97.94	97.59	97.60	98.39	97.43	97.54	98.09	97.48
	Mineral formula calculated on the basis of 23 oxygens											
Si-------	6.221	6.225	6.185	6.158	6.094	6.211	6.232	6.189	6.261	6.193	6.251	6.227
Al^{IV}-----	1.779	1.775	1.815	1.842	1.906	1.789	1.768	1.811	1.739	1.807	1.749	1.773
ΣTet-----	8.000	8.000	8.000	8.000	8.000	8.000	8.000	8.000	8.000	8.000	8.000	8.000
Al^{VI}-----	.253	.210	.257	.138	.225	.184	.178	.148	.285	.246	.288	.266
Fe^{2+}-----	.735	.791	.744	.705	.763	.720	.692	.705	.729	.782	.715	.733
Mg-------	3.514	3.529	3.516	3.524	3.417	3.451	3.507	3.497	3.526	3.570	3.527	3.491
Mn-------	.010	.012	.010	.009	.012	.009	.010	.010	.007	.010	.007	.009
Ti-------	.356	.353	.358	.456	.450	.463	.467	.475	.338	.337	.323	.348
Cr-------	.160	.167	.164	.162	.151	.155	.164	.161	.163	.157	.170	.178
ΣOct-----	5.029	5.062	5.048	4.994	5.019	4.983	5.017	4.996	5.048	5.102	5.030	5.025
Excess Oct	.029	.062	.048	.000	.019	.000	.017	.000	.048	.102	.030	.025
Ca-------	1.836	1.823	1.856	1.860	1.837	1.829	1.852	1.821	1.827	1.819	1.851	1.832
Na_B------	.135	.114	.096	.140	.144	.171	.131	.179	.125	.079	.119	.142
ΣB-------	2.000	2.000	2.000	2.000	2.000	2.000	2.000	2.000	2.000	2.000	2.000	2.000
Na_A------	.660	.684	.674	.664	.619	.614	.528	.628	.597	.687	.632	.645
K--------	.127	.122	.100	.114	.155	.114	.095	.112	.142	.122	.134	.131
ΣA site--	.787	.806	.773	.779	.774	.728	.623	.739	.739	.809	.765	.776
$Mg/(Mg+Fe^{2+})$	.83	.82	.83	.83	.82	.83	.84	.83	.83	.82	.83	.83
Accept[1]--	yes	yes	yes	yes	yes	no	yes	yes	yes	yes	yes	yes
Name-----	Pargasite	Pargasite	Pargasite	Pargasite	Pargasite	Pargasite	Pargasite	Pargasite	Pargasitic hornblende	Pargasite	Pargasitic hornblende	Pargasite

Table 7. Electron microprobe analyses and calculated mineral formulas of zoned amphibole crystals from the olivine cumulate of cyclic unit 2, Stillwater Complex, Montana—*Continued*

	755ca-pt3	755ca-pt14	830a-pt1	830a-pt2	830a-pt3	830a-pt10	830a-pt15	830a-pt6	830a-pt7	830a-pt8	830a-pt11
Microprobe analyses, weight percent											
SiO_2-----	43.2	43.6	42.9	42.9	43.0	42.6	42.7	42.7	43.0	42.4	42.8
Al_2O_3----	11.5	11.9	11.8	11.9	12.4	12.5	12.2	12.3	12.0	12.4	12.2
FeO------	6.0	6.2	6.1	6.3	5.6	5.7	5.7	6.1	6.0	6.2	5.9
Mgo------	16.3	16.4	16.5	16.7	16.5	16.4	16.4	16.4	16.5	16.5	16.4
MnO------	.07	.07	.07	.08	.07	.05	.06	.07	.09	.07	.07
TiO_2-----	3.4	3.3	3.0	3.1	3.5	3.0	3.1	2.8	2.6	2.8	2.9
CaO------	11.9	11.8	11.9	11.6	12.2	12.2	12.0	12.1	11.9	12.0	12.0
Na_2O-----	2.8	2.8	2.6	2.6	2.5	2.6	2.5	2.6	2.7	2.6	2.6
K_2O------	.72	.72	.97	.89	.96	.97	1.0	.93	.85	.91	.91
Cr_2O_3----	1.6	1.5	1.4	1.3	1.7	1.4	1.5	1.6	1.5	1.6	1.5
Total--	97.49	98.29	97.24	97.37	98.43	97.42	97.16	97.60	97.14	97.48	97.28
Mineral formula calculated on the basis of 23 oxygens											
Si-------	6.243	6.255	6.226	6.215	6.154	6.170	6.187	6.188	6.236	6.154	6.197
Al^{IV}-----	1.756	1.745	1.774	1.785	1.846	1.830	1.813	1.812	1.764	1.846	1.803
ΣTet-----	8.000	8.000	8.000	8.000	8.000	8.000	8.000	8.000	8.000	8.000	8.000
Al^{VI}-----	.206	.264	.253	.254	.249	.295	.277	.293	.290	.278	.287
Fe^{2+}-----	.722	.737	.739	.765	.672	.685	.695	.733	.728	.747	.717
Mg-------	3.519	3.497	3.566	3.600	3.525	3.543	3.541	3.534	3.569	3.555	3.549
Mn-------	.009	.009	.009	.010	.008	.006	.007	.009	.011	.009	.009
Ti-------	.374	.354	.323	.334	.374	.328	.338	.301	.287	.303	.314
Cr-------	.181	.168	.164	.143	.195	.165	.176	.179	.172	.180	.176
ΣOct-----	5.010	5.029	5.054	5.107	5.023	5.022	5.035	5.048	5.057	5.072	5.052
Excess Oct	.010	.029	.054	.107	.023	.022	.035	.048	.057	.072	.052
Ca-------	1.845	1.819	1.851	1.807	1.870	1.885	1.860	1.878	1.853	1.869	1.859
Na_B------	.145	.152	.096	.086	.108	.093	.105	.074	.090	.059	.089
ΣB-------	2.000	2.000	2.000	2.000	2.000	2.000	2.000	2.000	2.000	2.000	2.000
Na_A------	.634	.626	.625	.642	.587	.628	.600	.642	.661	.672	.633
K--------	.133	.132	.180	.165	.175	.179	.189	.172	.157	.168	.168
ΣA site--	.767	.758	.805	.806	.762	.807	.789	.814	.818	.840	.801
$Mg/(Mg+Fe^{2+})$	.83	.83	.82	.84	.84	.84	.84	.83	.83	.83	.83
Accept[1]--	yes	yes	yes	yes	yes	yes	yes	yes	yes	yes	yes
Name-----	Pargasite	Pargasitic hornblende	Pargasite	Pargasite	Pargasite	Pargasite	Pargasite	Pargasite	Pargasite	Pargasite	Pargasite

[1]Accepted, if:

1. Sum of tetrahedral sites = 8 ±0.02
2. Sum of octahedral sites >4.98
3. Excess octahedral site occupancy +Ca ≤2.02
4. Sum B site=2 ±0.0.2
5. Sum A site ≤1.02
6. Residual charge <0.02

Table 8. Electron microprobe analyses and calculated mineral formulas of chromite from the olivine cumulate of cyclic unit 2, Stillwater Complex, Montana
[Analyst: M.L. Zientek]

	Microprobe analyses, weight percent								
	747b core	747b rim a	747b rim 4	755 sp 1 core	755 sp 1 rim	830a sp 1	830a sp 2	830a sp 3	830a sp 4
SiO_2	0.03	0.09	1.3	0.00	0.01	0.00	0.00	0.00	0.00
Al_2O_3	18.5	18.6	18.1	16.6	16.6	20.4	19.9	20.5	20.0
Fe_2O_3	10.1	10.2	10.7	11.6	11.3	8.6	9.2	9.1	9.9
TiO_2	1.6	1.5	1.6	2.2	2.0	.76	.94	.82	.82
Cr_2O_3	37.1	36.9	36.2	36.6	36.4	37.3	37.2	36.9	36.5
FeO	23.6	22.7	22.3	25.2	25.1	23.1	23.5	23.0	23.7
MnO	.37	.38	.39	.44	.40	.33	.34	.34	.33
MgO	8.4	8.7	8.8	7.0	7.00	8.4	8.3	8.6	8.3
CaO	.00	.02	.04	.00	.08	.00	.00	.00	.00
Total	99.70	99.09	99.43	99.64	98.89	98.89	99.38	99.26	99.55

	Mineral formula based on 4 oxygens																	
	747b core		747b rim a		747b rim 4		755 sp 1 core		755 sp 1 rim		830a sp 1		830a sp 2		830a sp 3		830a sp 4	
Si	0.001		0.029		0.042		0.000		0.000		—		—		—		—	
Al	.731		.720		.705		.665		.669		0.793		0.775		0.796		0.777	
Fe^{3+}	.254	2.000	.255	2.000	.269	2.000	.297	2.000	.295	2.000	.215	2.000	.231	2.000	.226	2.000	.248	2.000
Ti	.040		.038		.040		.056		.053		.019		.023		.020		.020	
Cr	.974		.958		.944		.982		.983		.973		.971		.958		.955	
Fe^{2+}	.661		.629		.621		.723		.725		.643		.656		.640		.663	
Mn	.010	1.088	.010	1.068	.010	1.068	.012	1.093	.012	1.095	.010		.008		.010		.010	
Mg	.417		.429		.435		.358		.356		.418	1.071	.413	1.077	.427	1.077	.413	1.086
Ca	.000		.000		.002		.000		.002		—		—		—		—	
$Mg/(Mg+Fe^{2+})$	.387		.405		.412		.331		.329		.394		.386		.400		.384	
$Fe^{2+}/(Fe^{2+}+Fe^{3+})$	.722		.711		.698		.709		.711		.750		.740		.739		.728	
$Cr/(Cr+Al)$	.571		.571		.572		.596		.595		.551		.556		.546		.551	
$Fe^{3+}/(Cr+Al+Fe^{3+})$	.130		.132		.140		.153		.151		.108		.117		.114		.125	

distinctly higher in the chromite-bearing assemblage in sample 747b than for sample 755c and slightly higher for the chromite-bearing assemblage in sample 830a than for sample 755c. Similar variability is encountered for the Al^{IV}, Al^{VI}, and $(Na, K)_A$ contents in the hornblendes.

The variation between samples may in part reflect the composition of the phases coexisting with the brown hornblendes. Within the three samples studied, the amount of Ti in the hornblende formulas appears to correlate with the amount of Ti in the chromite formulas; however, the amount of Cr in the hornblendes does not correlate with the formula amounts of Cr in the chromites (fig. 13).

In summary, assemblage-controlled compositional variations in hornblende account for some of the variability seen in the hornblende analyses, such as with hornblendes in the chromite-absent interval in subunit 9 and with the Ti contents of hornblendes associated with chromite. However, variations in other compositional components do not appear to be systematically related to the crystalline assemblage coexisting with the hornblendes.

VARIATION IN HORNBLENDE COMPOSITION WITH STRATIGRAPHIC POSITION

A true average composition of hornblende at any particular stratigraphic position is difficult to obtain because, as has been shown previously, the hornblende composition is variable on a thin-section scale and in part depends upon the minerals with which it is in contact.

Nevertheless, arithmetical averages of selected properties of the hornblende analyses are plotted as a function of stratigraphic position (fig. 14), along with arithmetical averages of selected properties of hornblende analyses for different associated assemblage groups. Examining the overall patterns, especially for $Mg/(Mg + Fe^{2+})$, we see that the olivine cumulate package of cyclic unit 2 can be divided into three parts.

The lower part contains grain-size subunits 1, 2, 3, and 4 and is characterized by an average value of $Mg/(Mg + Fe^{2+})$ of approximately 0.82. Although the average Mg/(Mg

Table 9. Electron microprobe analyses and calculated mineral formulas of olivine from the olivine cumulate of cyclic unit 2, Stillwater Complex, Montana
[Analyst: M.L. Zientek. Al_2O_3, TiO_2, Cr_2O_3, and CaO were not detected]

	Microprobe analyses, weight percent					
	747b		755c		830a	
SiO_2	39.5		39.3		39.4	
FeO	14.7		14.5		14.4	
MnO	0.20		0.23		0.21	
MgO	45.7		45.5		45.8	
Total	100.10		99.53		99.81	
	Mineral formula based on 4 oxygens					
Si	0.990		0.990		0.990	
Fe	.308		.306		.301	
Mn	.004	2.020	.004	2.010	.004	2.015
Mg	1.708		1.710		1.714	
$Mg/(Mg+Fe^{2+})$	.85		.85		.85	

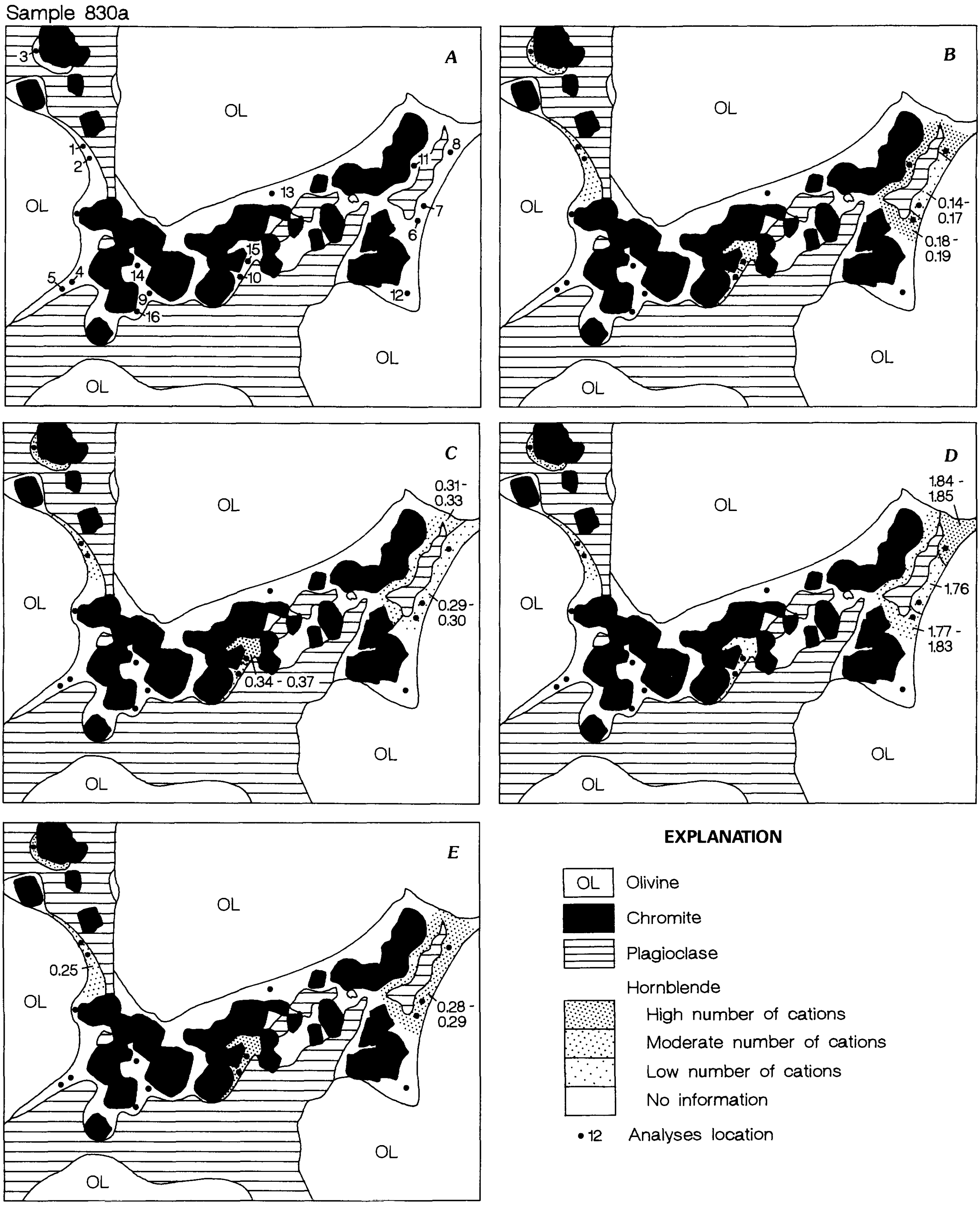

Figure 12. Sketches of compositional variation in zoned hornblendes of samples 830a, 747b, and 755c. *A*, Locations of points analyzed. *B*, Distribution of Cr cations per 23 oxygens. *C*, Distribution of Ti cations per 23 oxygens. *D*, Distribution of Al^{IV} cations per 23 oxygens. *E*, Distribution of Al^{VI} per 23 oxygens.

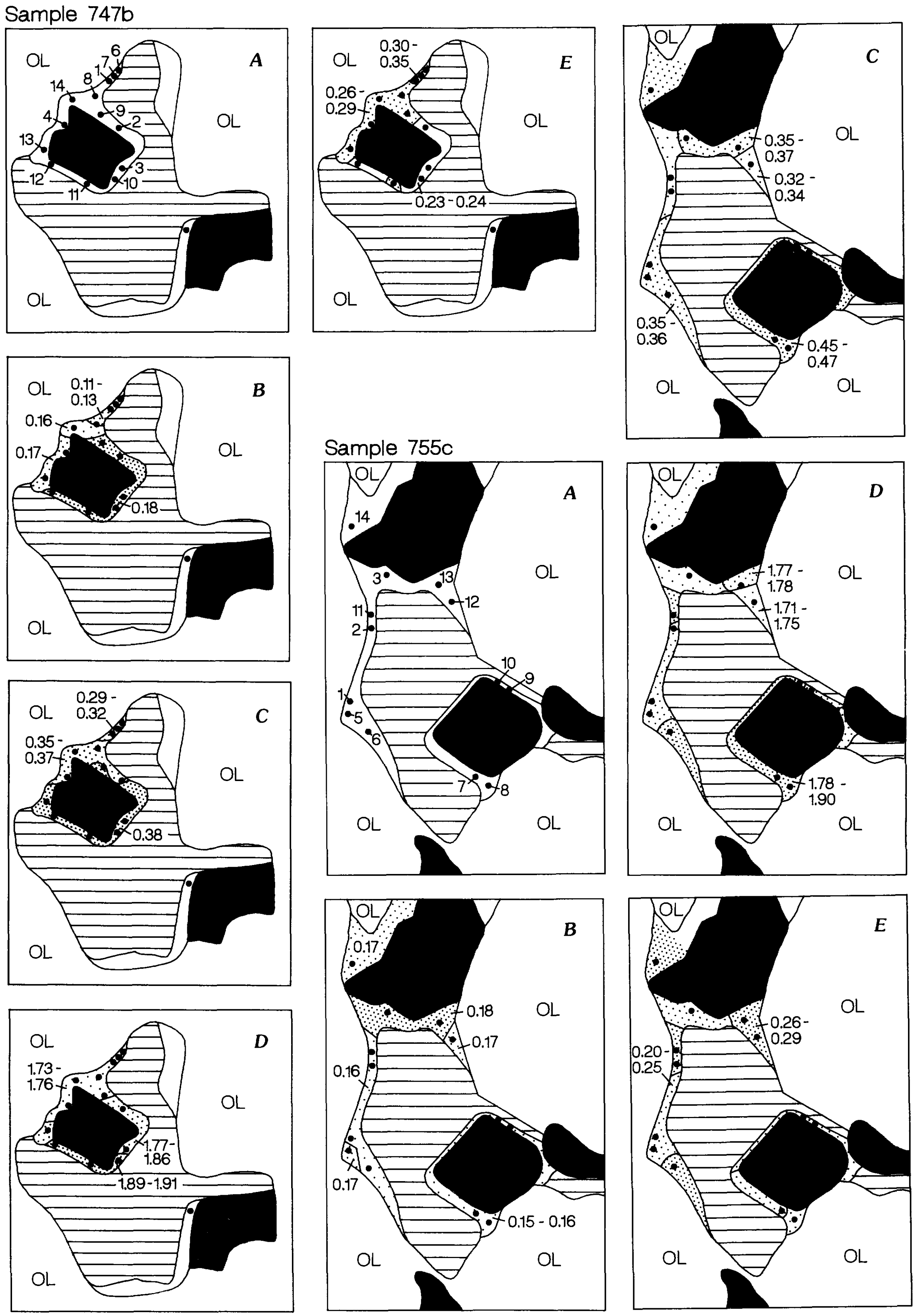

Figure 12. Continued.

+ Fe^{2+}) (fig. 14*B*) trends are quite complex and show increasing and decreasing trends with one discontinuity, the trend of Mg/(Mg + Fe^{2+}) for hornblendes associated with chromite and plagioclase (fig. 14*C*) is much simpler. The Mg/(Mg + Fe^{2+}) trend of hornblende associated with chromite and plagioclase is nearly constant; the compositional discontinuity between grain-size subunits 2 and 3 seen in figure 14*B* is not present. The slight iron-enrichment trends at the base of grain-size subunit 1 and the tops of subunits are still apparent. The compositional trend of Mg/(Mg + Fe^{2+}) for hornblende associated with augite (fig. 14*D*) is complex; a compositional discontinuity is present between grain-size subunits 2 and 3, and the base of subunit 3 is characterized by a magnesium-enrichment trend in the hornblende compositions. These results indicate that many of the small-scale fluctuations in the overall pattern result from averaging ratios of Mg/(Mg + Fe^{2+}) that vary between different assemblages; the significance of the small-scale fluctuations can only be assessed when this information on assemblages is available. Overall, this lower part is characterized by increasing Ti and Cl contents with stratigraphic position (fig. 14*E*, *G*). The F contents (fig. 14*G*) are lower than the Cl contents and have an inverse relation to the distribution of Cl. Al^{VI} is quite variable within samples; the trend of the Al^{IV} contents is erratic but shows an overall increase in the lower unit (fig. 14*F*). Cr is nearly constant (fig. 14*E*).

The middle part of the olivine cumulate package of cyclic unit 2 contains grain-size subunits 5, 6, 7, and 8; the chromitites appear in subunits 5 and 6. This middle part has a slightly higher range of Mg/(Mg + Fe^{2+}), 0.83 to 0.84, than the lower part. The lack of samples prohibits any conclusive generalizations about trends within the subunits. The Cr and Ti values are erratic (in part as a result of local alteration to colorless amphibole); in general, the Ti contents increase upward in the middle unit, with a compositional discontinuity between the lower and the middle parts. Al^{IV} values are erratic but slightly higher than the lower part. Cl contents are lower than those in the lower grain-size subunits.

The upper part contains grain-size subunit 9; the lower portion of this subunit contains no cumulus chromite. The values of Mg/(Mg + Fe^{2+}) in hornblende are lower than in the other grain-size subunits and average 0.81. Both Cr and Ti increase upward in this part. A sharp compositional discontinuity in Mg/(Mg + Fe^{2+}), Cr, and Ti is present between grain-size subunits 8 and 9. Al^{IV} is erratic and slightly less than the middle part but similar to the values seen in grain-size subunit 3 (lower part). Cl values are quite high.

One sample (755c), contains the boundary between two grain-size subunits (4 and 5). This sample represents about 7 cm of pegmatitic olivine cumulate, overlain by 0.3 cm of chromite cumulate, and followed by 4.1 cm of olivine-chromite cumulate. The pegmatitic olivine cumulate contains cumulus olivine and postcumulus plagioclase, orthopyroxene, phlogopite, and hornblende. The chromite cumulate occurs in an olivine-chromite cumulate with postcumulus plagioclase, augite, orthopyroxene, and hornblende. It also contains accessory amounts of pyrrhotite, pentlandite, magnetite, and chalcopyrite. The overlying olivine-chromite cumulate contains postcumulus hornblende, plagioclase, and minor amounts of magnetite, pyrrhotite, and pentlandite. Selected properties of the hornblendes through this section are compared in table 10 based on analyses given in table 2. The largest changes in the hornblende composition cumulate and involve decreases in formula units of Al^{VI} and Cr and increases in the amount of Al^{IV} and formula units of Ti and K.

VARIATION IN PHLOGOPITE COMPOSITION WITH STRATIGRAPHIC POSITION

Selected compositional parameters of phlogopite are shown (fig. 15) as a function of stratigraphic position relative to the size-graded subunits of the olivine cumulate. Average and single-grain analyses have been used to construct the tentative trend lines. The overall pattern is erratic. Each size-graded subunit (fig. 15*A*), where the data are available, appears to have its own patterns of increasing and (or) decreasing Mg/(Mg + Fe^{2+}), Ti, and Cr with stratigraphic height. The overall average trend of Mg/(Mg + Fe^{2+}) × 100 in phlogopite for the olivine cumulate of cyclic unit 2 appears to increase slightly with stratigraphic height (fig. 15*B*). No overall pattern is suggested by the Ti and Cr data (fig. 15*C*, *D*). Cl is more abundant than F in the phlogopites, which is the same relation observed in the hornblendes. Phlogopites in grain-size subunit 3 and the base of grain-size subunit 5 contain higher concentrations of both Cl and F (fig. 15*E*).

The most striking feature about the compositional variations shown in figure 15*B–D* is the sympathetic variation of Cr with Ti and the antithetic variation of Mg/(Mg + Fe^{2+}) × 100 with both Cr and Ti. The coupled substitution involving Mg and Ti in the octahedral sites in the phlogopites discussed earlier would predict an antithetic relation between Mg/(Mg + Fe^{2+}) × 100 and Mg and Ti, and this suggests that a coupled substitution involving Cr and Mg in the octahedral sites of these phlogopites may also be operative. Such a substitution could take the forms Mg $\rightleftharpoons$ Cr or Mg + Si $\rightleftharpoons$ Cr + Al, analogous to the Ti substitution schemes.

COMPARISON OF TRACE ELEMENTS INFORMATION

The variation of whole-rock Cr concentration with stratigraphic position in the olivine cumulates is mainly a function of the amount of chromite (Page and others, 1972). The concentration of whole-rock Ti with the olivine cumulates has a more irregular distribution but can be generally correlated with the concentration of Cr. When the variation in the concentrations of Cr and Ti are compared in detail, there is a significant noncorrespondence of Cr and Ti abundances in grain-size subunit 3 (fig. 16). The concentration of Ti does closely correspond to the abundance of amphibole plus phlogopite in this unit. This suggests that the whole-rock Ti contents of these cumulates reflect the abundances of both chromite and hornblende plus biotite. In addition, these results suggest that the Ti contents of cumulates cannot necessarily be used to approximate the volume of trapped, interstitial material (for example, Irvine, 1980, fig. 15).

INTERPRETATIONS AND CONCLUSIONS

Experimental studies have shown that few compositional parameters of hornblende are affected by changes in the coexisting assemblage at constant temperature and pressure as long as the bulk composition is constant (Helz, 1973, 1982). The results of the present study generally support this finding. As noted previously, there are only very subtle changes in the composition of hornblende in different textural associations. In the olivine cumulates of subunits 1 through 8, the overall compositions of hornblendes that replace augite cannot be statistically discriminated from the compositions of hornblendes that rim chromite (table 5). All analyses of brown amphibole define a very narrow compositional range (fig. 3).

However, the presence of chromite does have a very slight effect on the composition of hornblende. The hornblendes in the lower part of subunit 9 are characterized by less extensive coupled substitution and lower amounts of Cr and Ti; cumulus chromite is absent from the rocks in this part of the subunit. In single thin sections, hornblendes associated with chromite exhibit a higher degree of coupled substitution. Within individual crystals, the proportions of Ti and to a lesser extent of Al^{IV} and Cr increase in abundance adjacent to chromite crystals (fig. 12). The Ti contents of these hornblendes are related to the Ti contents of the associated chromite (fig. 13). $Mg/(Mg + Fe^{2+})$ of the hornblendes is not significantly affected by the presence or absence of chromite.

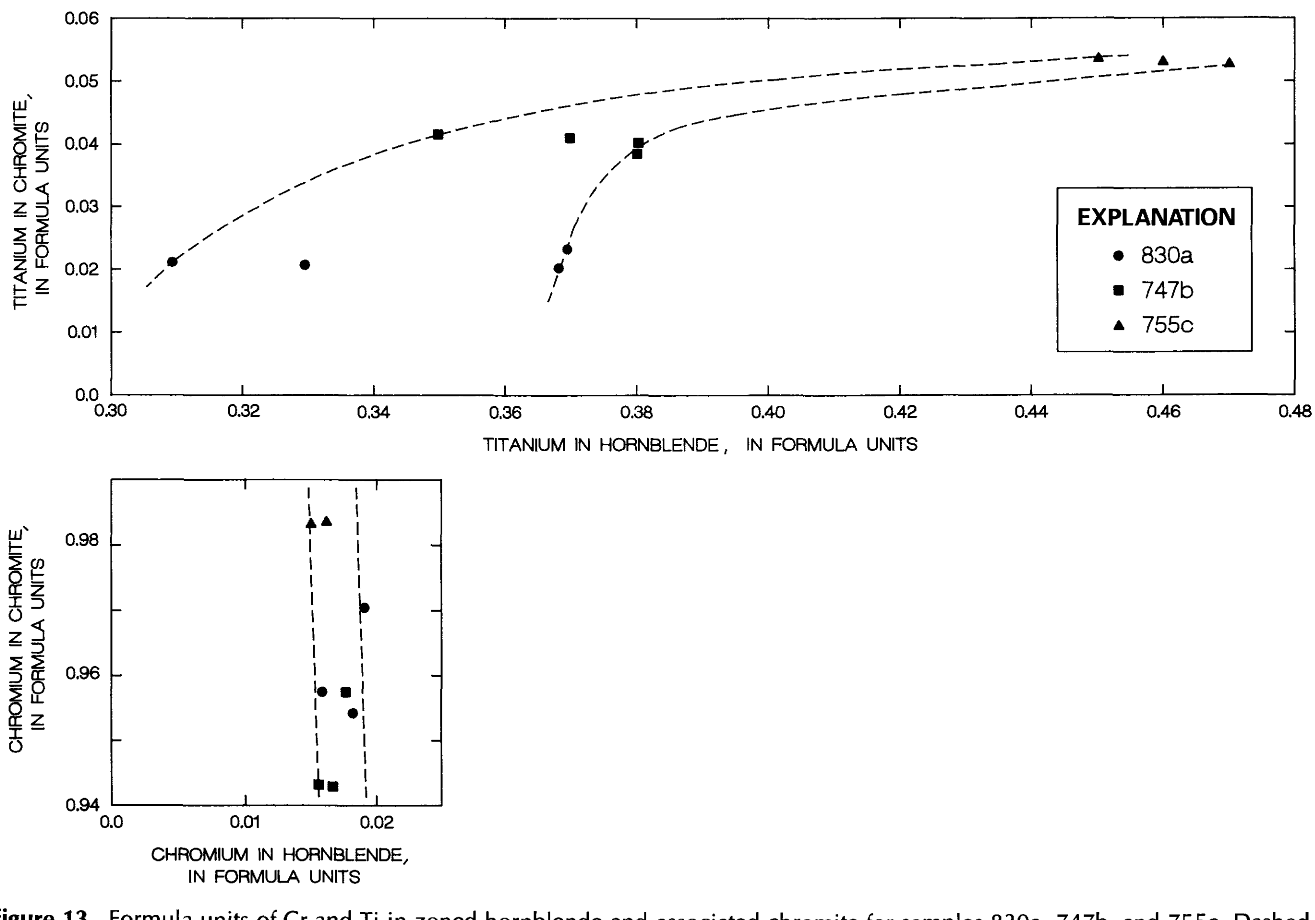

Figure 13. Formula units of Cr and Ti in zoned hornblende and associated chromite for samples 830a, 747b, and 755c. Dashed lines bound observed data.

These observations are also in accord with experimental observations. Helz (1973, 1982) has noted that the TiO_2 contents of hornblende are strongly affected by changes in the oxide assemblage. The compositions of the hornblendes in cyclic unit 2 are influenced by the local environment of crystallization.

Experimental studies by Helz (1973) demonstrated that the Al^{IV} and Ti contents of hornblende were strongly correlated with temperature. If the results from the QFM-buffered, 1921 Kilauea olivine tholeiite experiments are used to model the Stillwater magma, crystallization temperatures or (more likely) the blocking temperature can be estimated for the brown hornblendes. The estimated temperatures are summarized in table 11. Temperatures based upon the Al^{IV} contents of the hornblendes generally fall within a narrow range, 905 to 981 °C. The average temperature appears to be 930 °C. Difference in temperatures between different assemblages in the same thin section are less than the estimated difference based on analytical error. A range of temperatures within single hornblende crystals is recorded in samples 747b, 755c, and 830a. The temperatures are highest adjacent to chromite grains (approximately 980 °C) and are approximately 930 to 940 °C away from chromite. Temperatures based on the Ti contents of the hornblendes are much less systematic. Values range from 748 to 999 °C. The high and low temperatures given in these ranges do not correspond to the same analyzed points that give the maximum and minimum recorded temperatures based upon the Al^{IV} contents of the hornblendes. The Ti contents of the hornblendes in these rocks do not accurately reflect the temperatures at which they crystallized, because they did not crystallize in equilibrium with ilmenite.

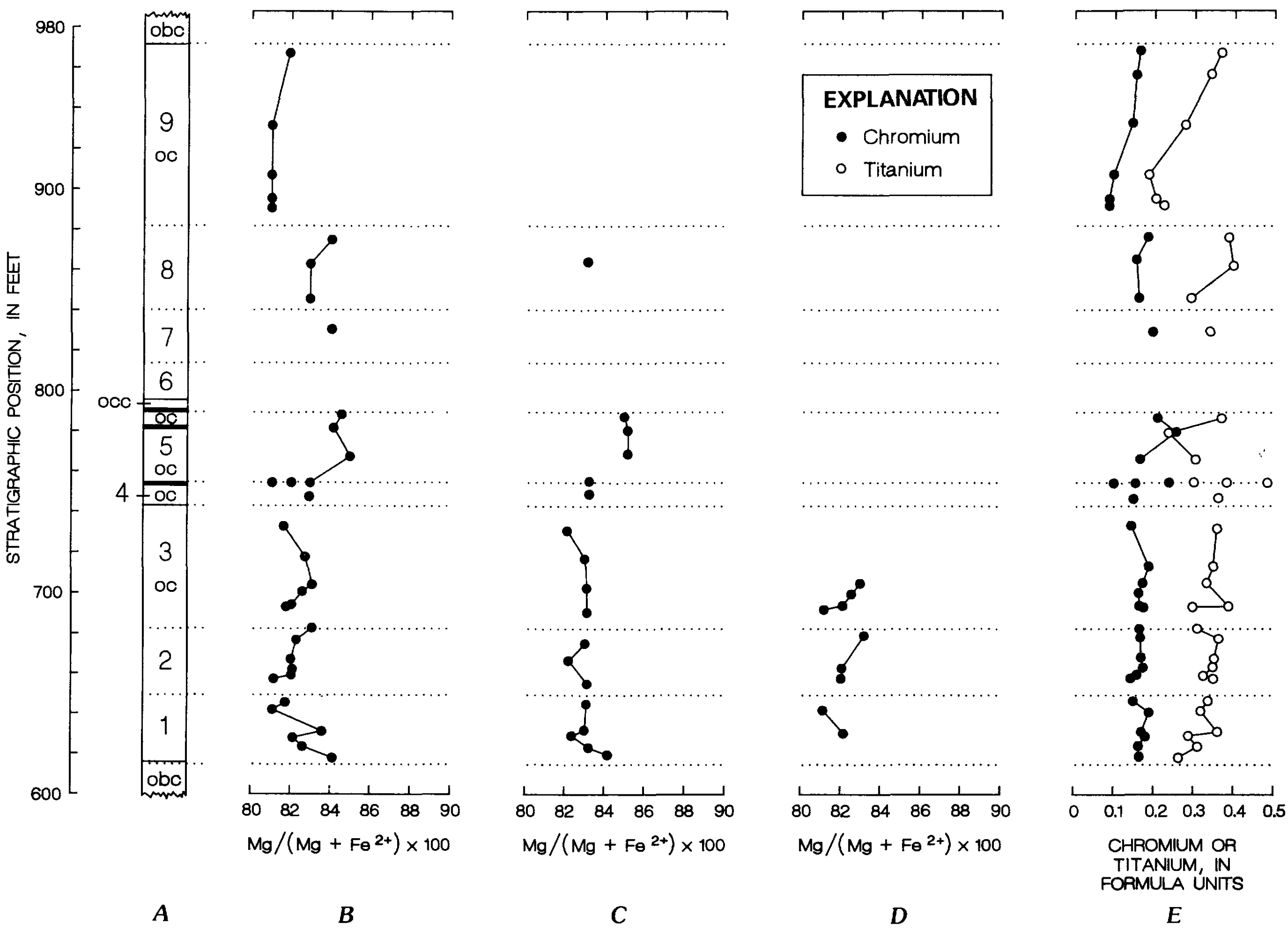

Figure 14. Variation in selected compositional properties of hornblende with stratigraphic position. *A*, Columnar section of olivine cumulate of cyclic unit 2, Stillwater Complex, Montana, with size-graded units (dotted lines) numbered; occ, olivine-chromite cumulate; oc, olivine cumulate; obc, olivine-bronzite cumulate; heavy lines, chromite cumulate. *B*, Arithmetical average of $Mg/(Mg + Fe^{2+}) \times 100$ in hornblende; analyses from table 2. *C*, Average $Mg/(Mg + Fe^{2+}) \times 100$ in hornblende associated with chromite and plagioclase. *D*, Average $Mg/(Mg + Fe^{2+}) \times 100$ of hornblende associated with augite. *E*, Average formula units of Cr and Ti in brown amphiboles from table 2. *F*, Al^{IV} in brown amphiboles. *G*, Average weight percent Cl and F in brown amphiboles.

The values of $Mg/(Mg + Fe^{2+})$ for the hornblendes vary only slightly but change systematically as a function of stratigraphic position. As noted previously, this change in hornblende composition can be correlated with changes in the mode and grain size of the olivine cumulates. In essence, the rocks below the chromite seams, the rocks associated with and slightly above the chromite seams, and the rocks within the chromite-free lower part of subunit 9 all have distinct amphibole compositions. The relative depletion of Cr in hornblendes above the chromite seams suggests that the processes responsible for chromite seam formation within the cumulates perhaps also influenced the composition of hornblendes that formed later.

The textural and chemical evidence indicate that the brown hornblendes crystallized from trapped interstitial liquid at high temperatures (in excess of 900 °C). Local variations in hornblende composition suggest that the local environment influenced the composition. The hornblendes that rim chromite may have formed earlier than the hornblendes that replace augite, because the highest recorded temperatures are from hornblendes immediately adjacent to chromite crystals. On average, about 96 percent of the interstitial space is occupied by plagioclase, augite, and orthopyroxene, all of which crystallized before or slightly overlapping the crystallization of hornblende and phlogopite. Although the quantitative relation between porosity and permeability is variable in both sandstones and cumulates, in general the higher the porosity, the greater is the permeability (Levorsen, 1958). Porosities of less than 5 percent in sandstones are associated with extremely low permeabilities (less than 0.1 millidarcy). Thus, the small volume of pore space left at the time of hornblende and phlogopite

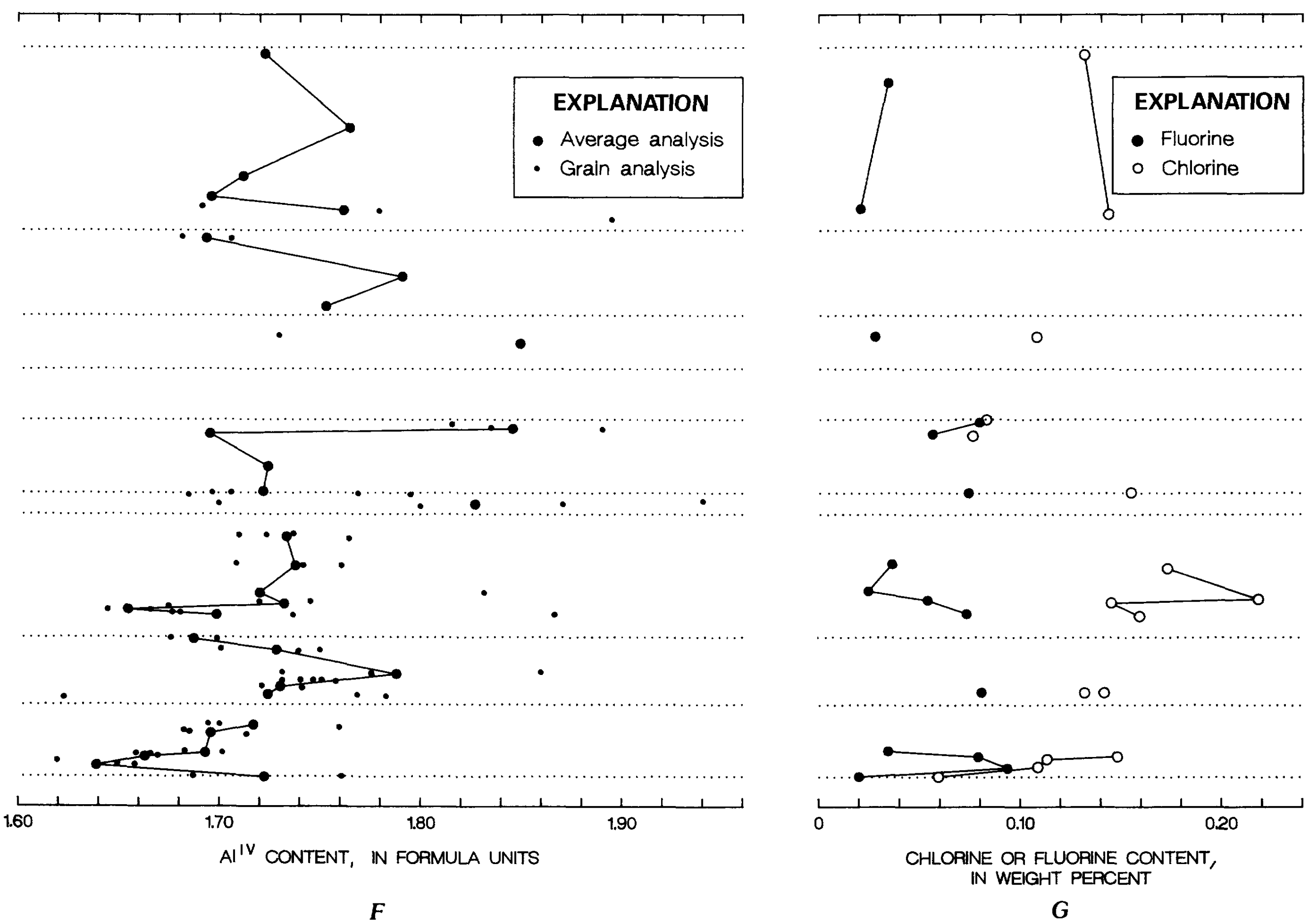

Figure 14. Continued.

Table 10. Comparison of selected compositional properties of brown amphiboles through a section of olivine cumulate containing a chromite cumulate, cyclic unit 2, Stillwater Complex, Montana

[oc, olivine cumulate; occ, olivine-chromite cumulate; cc, chromite cumulate]

Sample-----	755	755	755b
Rock-------	occ	occ	oc, cc
Al^{IV}-------	1.7	1.8	1.7
Al^{VI}-------	.28	.16	.27
A-site-----	.76	.70	.70
X_{Mg}--------	.83	.82	.81
X_{Ti}--------	.37	.50	.30
X_{Cr}--------	.16	.09	.24
X_K---------	.13	.20	.12
Na_4--------	.17	.18	.11

crystallization suggests that the permeability of the olivine cumulate was small. Apparently, large-scale movement of trapped residual liquid, which would completely homogenize the final compositions of hornblende, did not occur or had ceased by the time hornblende finally crystallized. This discussion does not confirm or deny the movement of residual liquids prior to the crystallization of hornblende. However, if the residual liquids were derived from the underlying cyclic unit, they would have been in equilibrium with both cumulus olivine and orthopyroxene before migration and probably should have made the compositions of the interstitial minerals in subunit 1 different from those in the succeeding two subunits, both in which the initial interstitial liquid would have been in equilibrium with olivine alone. There is little difference between subunit 1 and the next two overlying cyclic units, which suggests that residual liquids did not migrate very far even at the time when the porosity and permeability would have been relatively high.

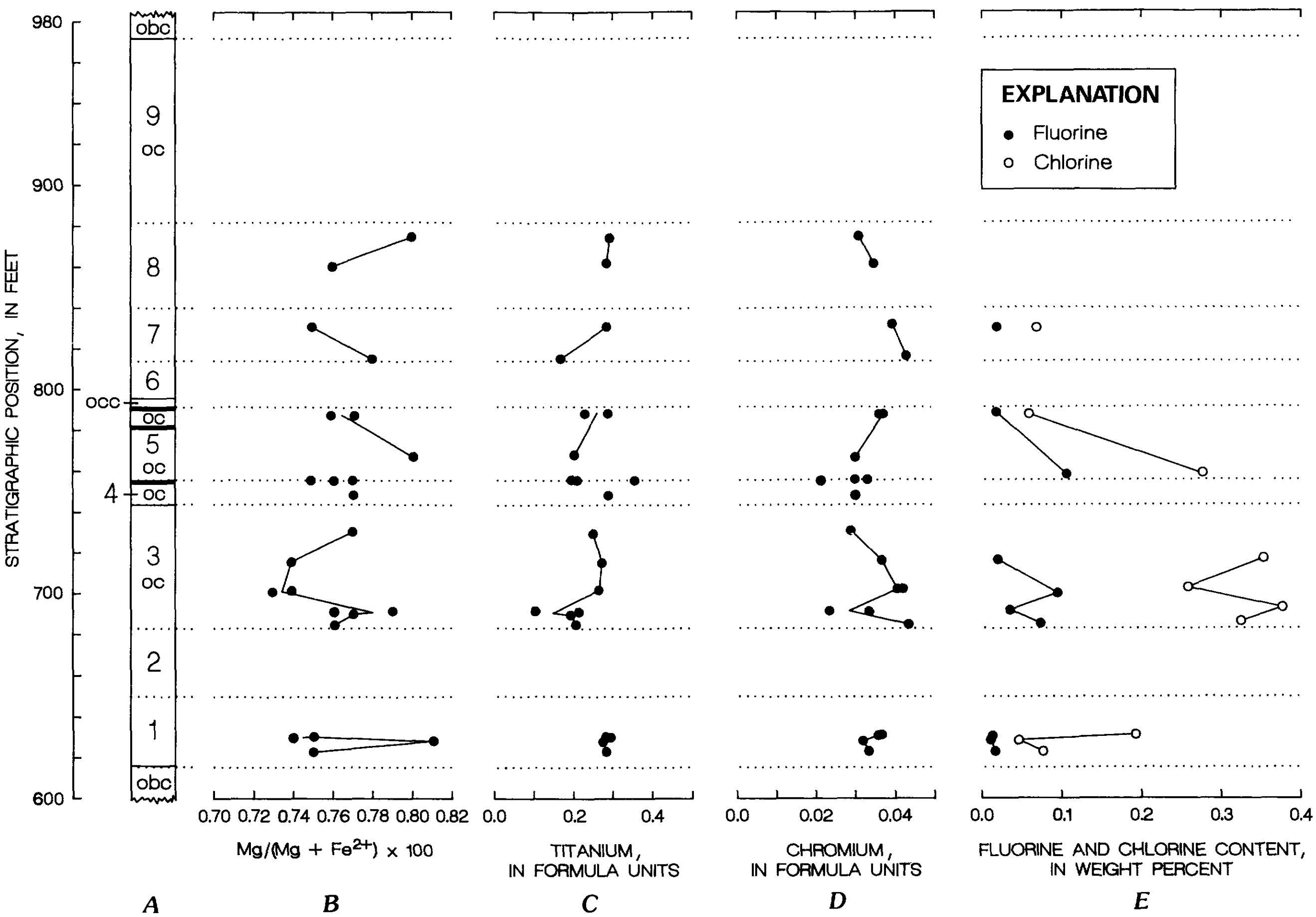

Figure 15. Variation in selected compositional properties of phlogopite with stratigraphic position. *A*, Columnar section of the olivine cumulate of cyclic unit 2, Stillwater Complex, Montana, with size-graded units (dotted lines) numbered. occ, olivine-chromite cumulate; oc, olivine cumulate; obc, olivine-bronzite cumulate; heavy lines, chromite cumulate. *B*, Mg/(Mg + Fe^{2+}) × 100 in phlogopite. *C*, Formula amounts of Ti in phlogopite. *D*, Formula amounts of Cr in phlogopite. *E*, Weight percent Cl and F in phlogopite.

The colorless tremolitic amphiboles formed later than the hornblendes and are generally associated with alteration that postdates final consolidation of the cumulates.

The phlogopites are compositionally homogeneous, varying only in the extent of Ti and Cr substitution in the octahedral sites. Experimental studies indicate that the Ti solubility in phlogopites is dependent on pressure, temperature, oxygen fugacity, and the bulk composition of the magma from which they crystallize (Arima and Edgar, 1981). Experimental studies that approximate the conditions at which the Stillwater Complex magma would have crystallized have not been done, nor has the extent of Cr solubility in phlogopite as a function of temperature, pressure, and bulk composition been determined. Therefore, at this time, it is not possible to estimate the changes in any of these parameters that would be necessary to produce the limited variations noted in this report. It can be stated, however, that the compositions of phlogopites from the olivine cumulate of cyclic unit 2 are closer to those of phlogopites from high-pressure experimental runs, from potassium mantle-derived rocks, and from potassium-rich rocks that crystallized at depth than to those of other rocks that crystallized at shallow depths (compare with Arima and Edgar, 1981). Nevertheless, the phlogopites certainly did not crystallize at high pressure and must have crystallized under conditions similar to those prevailing when hornblendes crystallized.

Finally, the Cl and F contents of both hornblende and phlogopite indicate that the magma from which they crystallized was not notably enriched in these elements. Many recent studies have suggested that volatiles in mafic magmas may play an important role in the concentration of platinum-group elements (Bow and others, 1982; Kinloch, 1982). Studies of platiniferous hortonolitic dunite pipes in the Bushveld Complex have shown that amphiboles are enriched in chlorine (0.41 to 0.83 weight percent; Schiffries, 1982) and phlogopites are enriched in fluorine (Wagner, 1929). The B-chromitite of cyclic unit 2 is enriched in platinum-group elements (Page and others, 1976); however, there is no indication that the Cl or F contents of the magma played a significant role in the concentration of platinum-group elements in this part of the Ultramafic series.

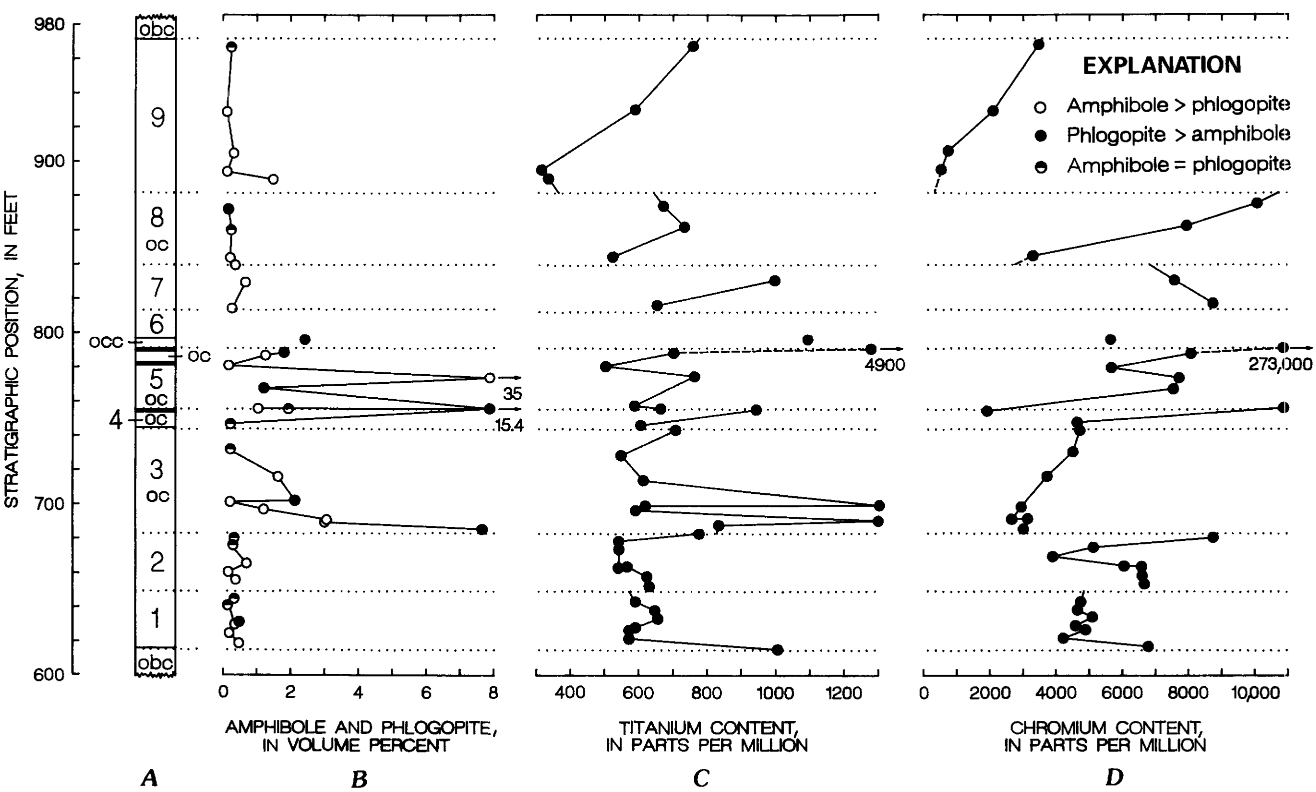

Figure 16. Trace-element variation in the olivine cumulates with stratigraphic position. *A*, Columnar section of the olivine cumulate of cyclic unit 2, Stillwater Complex, Montana, with size-graded units (dotted lines) numbered. occ, olivine-chromite cumulate; oc, olivine cumulate; obc, olivine-bronzite cumulate; heavy lines, chromite cumulate. *B*, Distribution of amphibole and biotite. *C*, Ti content. *D*, Cr content. Dashed lines represent values going off the scale.

Table 11. Estimated temperatures of brown amphibole crystallization based on experimental studies of the 1921 Kilauea olivine tholeiite (Helz, 1973)

[Estimated errors in temperature based on analytical methods are ±14 °C for the Al^{IV} estimates and ±35 °C for the Ti estimates. These results are based on one standard deviation determined for Al^{IV} and Ti for the standard (table 4)]

	Temperatures based on the Al^{IV} contents of the amphibole (°C)	Temperatures based on the Ti contents of the amphibole (°C)
Average composition of 32 amphiboles associated with spinel	938	932
Average composition of 15 amphiboles that replace clinopyroxene	923	918
Average composition of 5 amphiboles from unit 9 in which chromite is not present	930	784
Range of assemblages in sample 618	911–941	748–918
Range of assemblages in sample 640	905–923	862–918
Range of assemblages in sample 660	938–941	918–930
Range of assemblages in sample 690	905–916	840–918
Range of assemblages in sample 715	930–941	851–978
Range of assemblages in sample 787	954–976	930–976
Crystal zoning in sample 747	932–981	872–974
Crystal zoning in sample 755c	936–981	908–999
Crystal zoning in sample 830	941–966	870–971

REFERENCES CITED

Arima, M., and Edgar, A.D., 1981, Substitution mechanisms and solubility of titanium in phlogopites from rocks of probable mantle origin: Contributions to Mineralogy and Petrology, v. 77, p. 288–295.

Bow, C., Wolfrom, D., Turner, A., Barnes, S., Evans, J., Zdepski, M., and Boudreau, A., 1982, Investigations of the Howland Reef of the Stillwater Complex, Minneapolis Adit Area: Stratigraphy, structure and mineralization: Economic Geology, v. 77, p. 1481–1492.

Cameron, M., and Papike, J.J., 1979, Amphibole crystal chemistry: a review: Fortschritte Mineralogie, v. 57, p. 28–67.

Foster, M.D., 1960, Interpretation of the composition of trioctahedral micas: U.S. Geological Survey Professional Paper 354-B, p. 11–49.

Helz, R.T., 1973, Phase relations of basalts in their melting range at P_{H_2O} = 5 kb as a function of oxygen fugacity, Pt. 1, Mafic phases: Journal of Petrology, v. 14, p. 249–302.

——— 1982, Phase relations and compositions of amphiboles produced in studies of melting behavior of rocks, *in* Veblen, D.R., and Ribbe, P.H., eds., Amphiboles: Petrology and experimental phase relations: Mineralogical Society of America, Reviews in Mineralogy, v. 9B, p. 279–346.

Irvine, T.N., 1980, Magmatic infiltration metasomatism, double-diffusive fractional crystallization, and all cumulus growth in the Muskox intrusion and other layered intrusions, *in* Hargroves, R.B., ed., Physics of magmatic processes: Princeton, N. J., Princeton University Press, p. 327–383.

Jackson, E.D., 1961, Primary textures and mineral associations in the ultramafic zone of the Stillwater Complex, Montana: U.S. Geological Survey Professional Paper 358, 106 p.

——— 1963, Stratigraphic and lateral variation of chromite composition in the Stillwater Complex: Mineralogical Society of America Special Paper 1, p. 46–54.

——— 1967, Ultramafic cumulates in the Stillwater, Great Dyke, and Bushveld intrusions, *in* Wyllie, P. J., ed., Ultramafic and related rocks: New York, John Wiley, p. 20–38.

——— 1968, The chromite deposits of the Stillwater Complex, Montana, *in* Ore deposits of the United States, 1933–1967 (Graton-Sales Volume): New York, American Institute of Mining, Metallurgical, and Petroleum Engineers, v. 2, p. 1495–1510.

——— 1969, Chemical variation in coexisting chromite and olivine in chromitite zones of the Stillwater Complex (with discussion): Economic Geology, Monograph 4, p. 41–75.

——— 1970, The cyclic unit in layered intrusions, a comparison of repetitive stratigraphy in the ultramafic parts of the Stillwater, Muskox, Great Dyke, and Bushveld complexes (with discussion), *in* Bushveld igneous complex and other layered intrusions: Symposium, Geological Society of South Africa, Special Publication 1, p. 391–424.

——— 1971, The origin of ultramafic rocks by cumulus processes: Fortschritte Mineralogie, v. 48, p. 128–174.

Kinloch, E.D., 1982, Regional trends in the platinum-group mineralogy of the Critical zone of the Bushveld Complex, South Africa: Economic Geology, v. 77, p. 1328–1347.

Kretz, R., 1966, Interpretation of the shape of mineral grains in metamorphic rocks: Journal of Petrology, v. 7, p. 68–94.

Leake, B.E., 1978, Nomenclature of amphiboles: American Mineralogist, v. 63, p. 1023–1052.

Levorsen, A.I., 1958, Geology of petroleum: San Francisco, W. H. Freeman, 703 p.

Page, N.J, 1976, Serpentinization and alteration in an olivine cumulate from the Stillwater Complex, southwestern Montana: Contributions to Mineralogy and Petrology, v. 54, no. 2, p. 127–137.

Page, N.J, Rowe, J.J., and Haffty, J., 1976, Platinum metals in the Stillwater Complex, Montana: Economic Geology, v. 71, no. 7, p. 1352–1363.

Page, N.J, Shimek, R., and Huffman, C., Jr., 1972, Grain-size variations within an olivine cumulate, Stillwater Complex, Montana: U.S. Geological Survey Professional Paper 800–C, p. C29–C37.

Papike, J.J., Cameron, K L., and Baldwin, K., 1974, Amphiboles and pyroxenes: Characterization of other than quadrilateral components and estimates of ferric iron from microprobe data [abs.]: Geological Society of America Abstracts with Programs, v. 6, p. 1053–1054.

Raedeke, L.D., 1982, Petrogenesis of the Stillwater Complex: Seattle, Wash., University of Washington, Ph.D. dissertation, 212 p.

Raedeke, L.D., and McCallum, I.S., 1982a, Modal and chemical variations in the ultramafic zone of the Stillwater Complex, *in* Walker, D., and McCallum, I.S., eds., Workshop on magmatic processes of early planetary crusts: Magma oceans and stratiform layered intrusions: Houston, Tex., Lunar and Planetary Institute, LPI Technical Report 82-01, p. 135–137.

——— 1982b, Field guide to the Stillwater Complex, *in* Walker, D., and McCallum, I.S., eds., Workshop on magmatic processes of early planetary crusts: Magma oceans and stratiform layered intrusions: Houston, Tex., Lunar and Planetary Institute, LPI Technical Report 82-01 p. 169–194.

——— 1984, Investigations in the Stillwater Complex: Part II. Petrology and petrogenesis of the Ultramafic series: Journal of Petrology, v. 25, p. 395–420.

Schiffries, C.M., 1982, The petrogenesis of a platiniferous dunite pipe in the Bushveld Complex: Infiltration metasomatism by a chloride solution: Economic Geology, v. 77, p. 1439–1453.

Wagner, P.A., 1929, The platinum deposits and mines of South Africa: Edinburgh, Scotland, Oliver and Boyd, 321 p.

Wones, D.R., and Gilbert, M.C., 1982, Amphiboles in the igneous environment, *in* Veblen, D.R., and Ribbe, P.H., eds., Amphiboles: Petrology and experimental phase relations: Mineralogical Society of America, Reviews in Mineralogy, v. 9B, p. 355–390.

Yakowitz, H., Myklebust, R.L., and Heinrich, K.F.J., 1973, FRAME: an on-line correction procedure for quantitative electron microprobe analyses: National Bureau of Standards Technical Note 796, 46 p.

Zientek, M.L., Czamanske, G.K., and Irvine, T.N., 1985, Stratigraphy and nomenclature for the Stillwater Complex: Montana Bureau of Mines Special Publication 92, p. 21-32.